Universiteit Leiden
Leiden Observatory

Elena Maria Rossi

Sjoert van Velzen

First **observational constraints** on the **GW-AGN connection** through **spatial correlation** analysis

The most luminous AGN do not produce the majority of the detected stellar-mass Black Hole Binary mergers in the local Universe

Niccolò Veronesi - Belgian-Dutch Gravitational Wave Meeting 2023 - 23/10/2023

The most luminous AGN do not produce the majority of the detected stellar-mass black hole binary mergers in the local Universe

Niccolò Veronesi,[1]★ Elena Maria Rossi,[1] Sjoert van Velzen,[1]
[1] *Leiden Observatory, Leiden University, PO Box 9513, 2300 RA Leiden, The Netherlands*

Accepted 2023 October 12. Received 2023 September 15; in original form 2023 June 19

ABSTRACT
Despite the increasing number of Gravitational Wave (GW) detections, the astrophysical origin of Binary Black Hole (BBH) mergers remains elusive. A promising formation channel for BBHs is inside accretion discs around supermassive black holes, that power Active Galactic Nuclei (AGN). In this paper, we test for the first time the spatial correlation between observed GW events and AGN. To this end, we assemble all sky catalogues with 1,412 (242) AGN with a bolometric luminosity greater than $10^{45.5}$erg s^{-1} (10^{46} erg s^{-1}) with spectroscopic redshift of $z \leq 0.3$ from the Milliquas catalogue, version 7.7b. These AGN are cross-matched with localisation volumes of BBH mergers observed in the same redshift range by the LIGO and Virgo interferometers during their first three observing runs. We find that the fraction of the detected mergers originated in AGN brighter than $10^{45.5}$ erg s^{-1} (10^{46} erg s^{-1}) cannot be higher than 0.49 (0.17) at a 95 per cent credibility level. Our upper limits imply a limited BBH merger production efficiency of the brightest AGN, while most or all GW events may still come from lower luminosity ones. Alternatively, the AGN formation path for merging stellar-mass BBHs may be actually overall subdominant in the local Universe. To our knowledge, ours are the first observational constraints on the fractional contribution of the AGN channel to the observed BBH mergers.

How can we learn where BBHs merge?

INARY LACK OLE

How can we learn where BBHs merge?

INARY LACK OLE

Detection of
ElectroMagnetic
transient **counterparts**

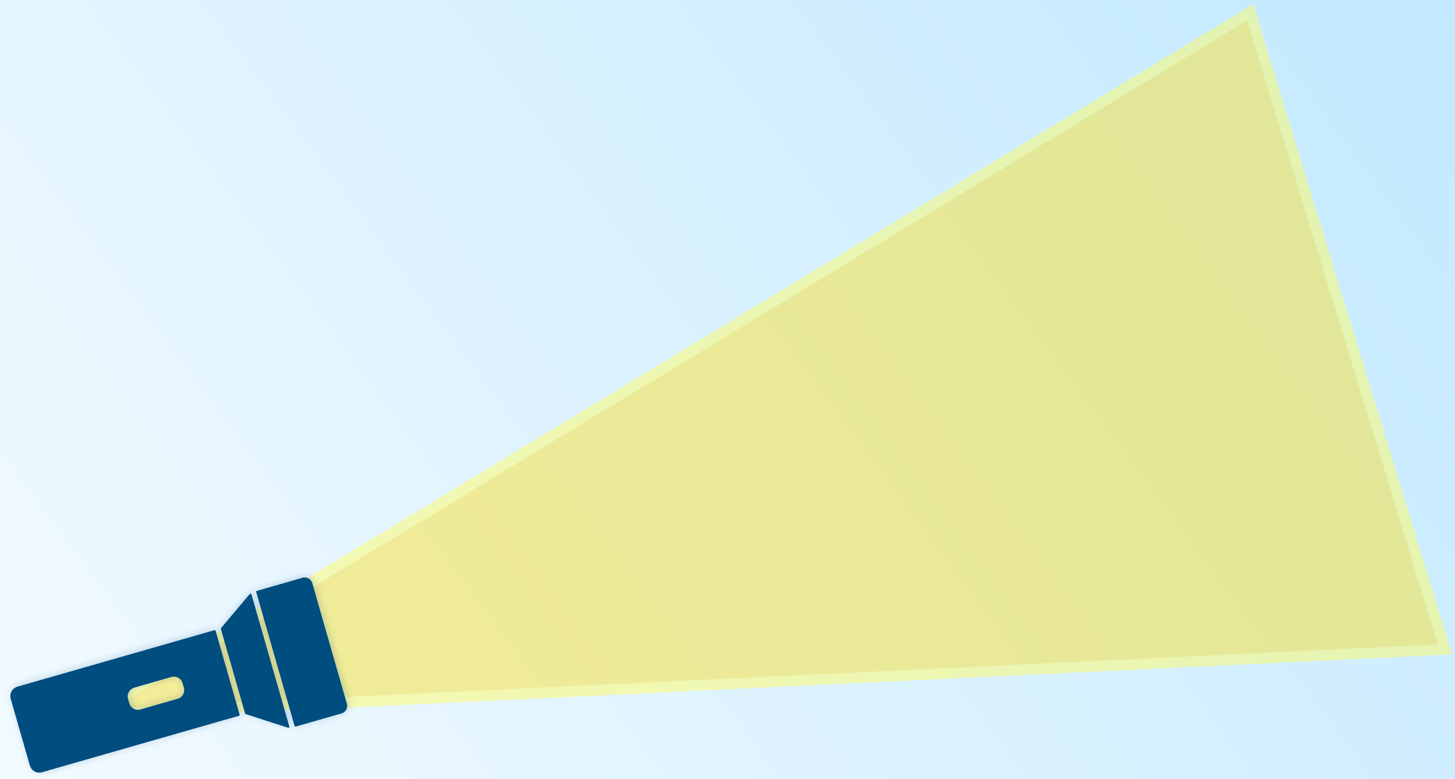

Graham+20, Graham+23, Ashton+21

How can we learn where BBHs merge?

INARY LACK OLE

Detection of **ElectroMagnetic** transient **counterparts**

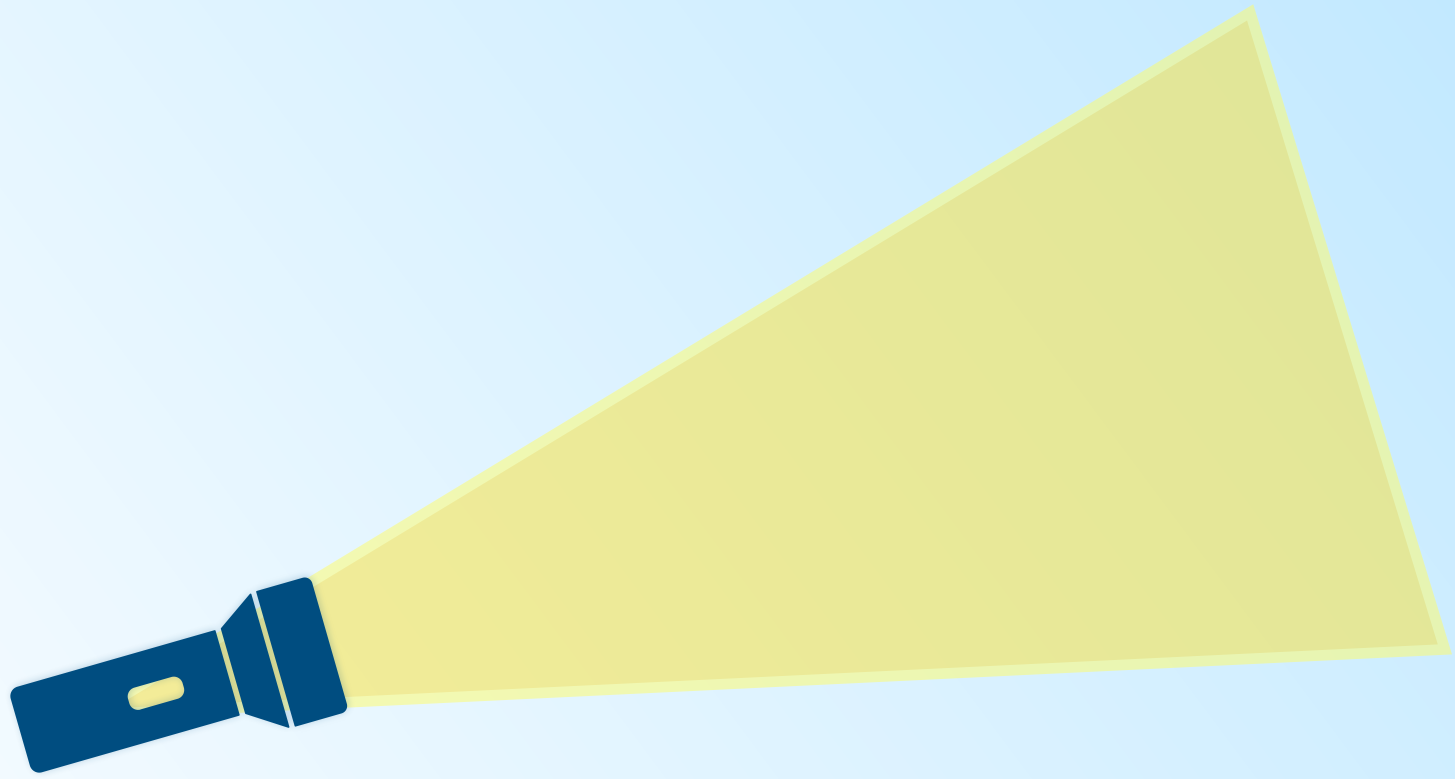

Graham+20, Graham+23, Ashton+21

Predictions on **binary parameters** and **comparison** to **observations**

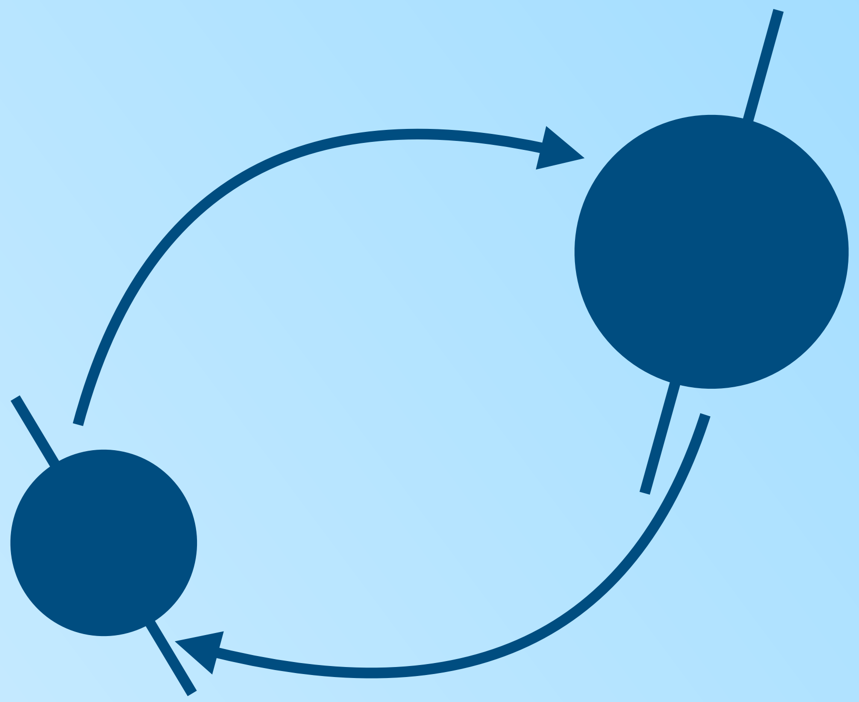

McKernan+20, Romero-Shaw+21,
Gayathri+21, Karathanasis+22, …

How can we learn where BBHs merge?

INARY LACK OLE

Detection of **ElectroMagnetic** transient **counterparts**

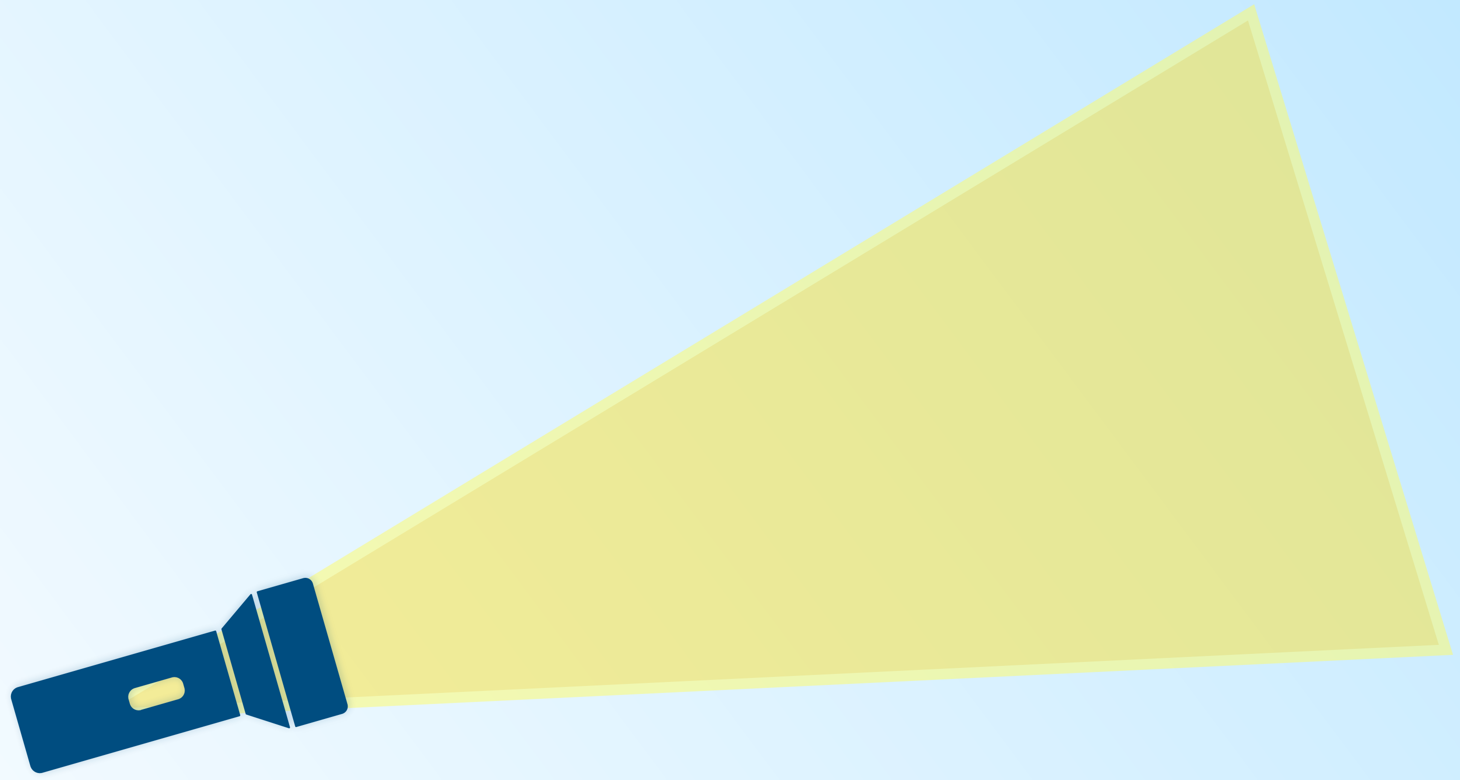

Graham+20, Graham+23, Ashton+21

Predictions on **binary parameters** and **comparison** to **observations**

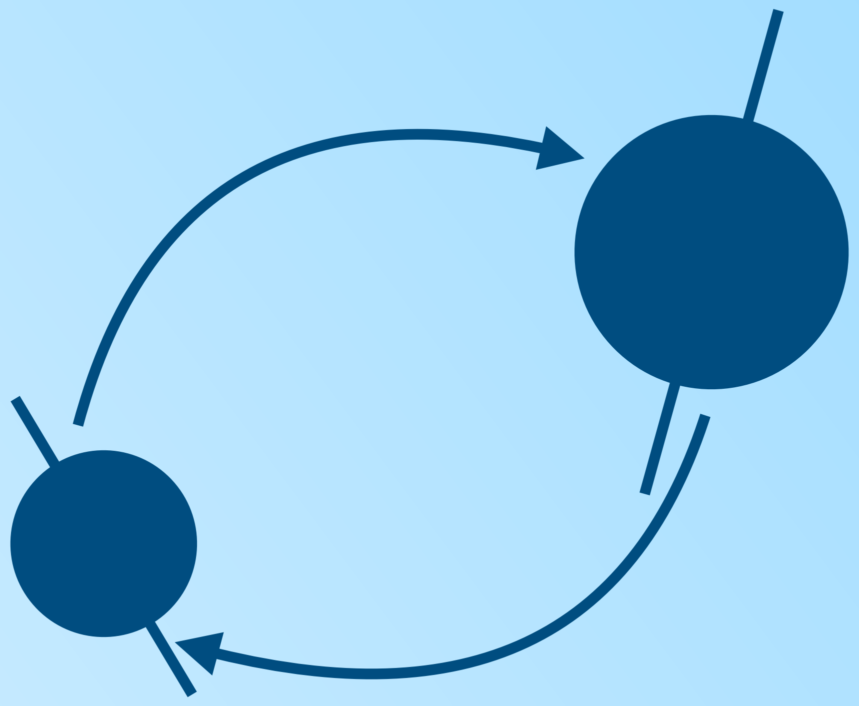

McKernan+20, Romero-Shaw+21, Gayathri+21, Karathanasis+22, …

Investigation of **spatial correlation** with potential hosts

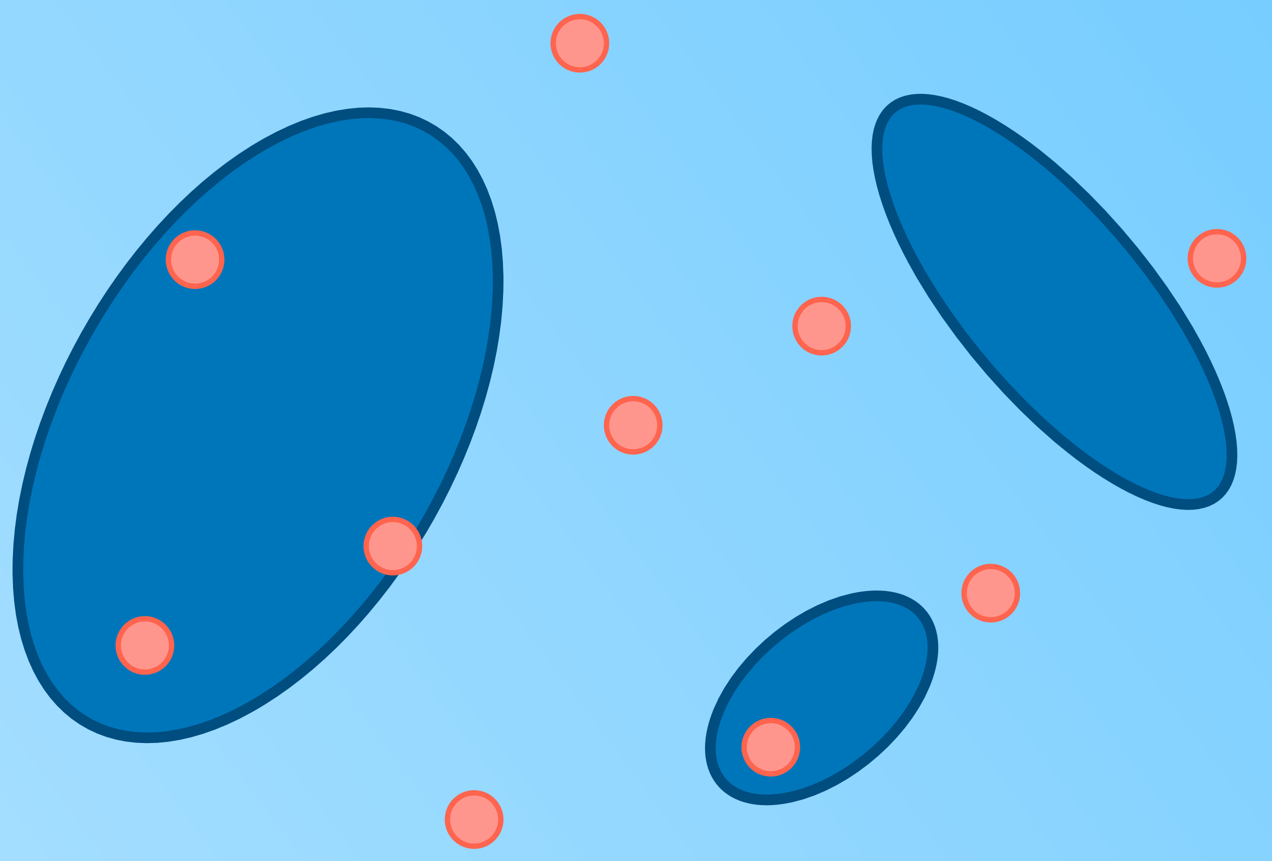

Bartos+17, Corley+19, NV+22, NV+23

How can we learn where BBHs merge?

INARY LACK OLE

Detection of **ElectroMagnetic** transient **counterparts**

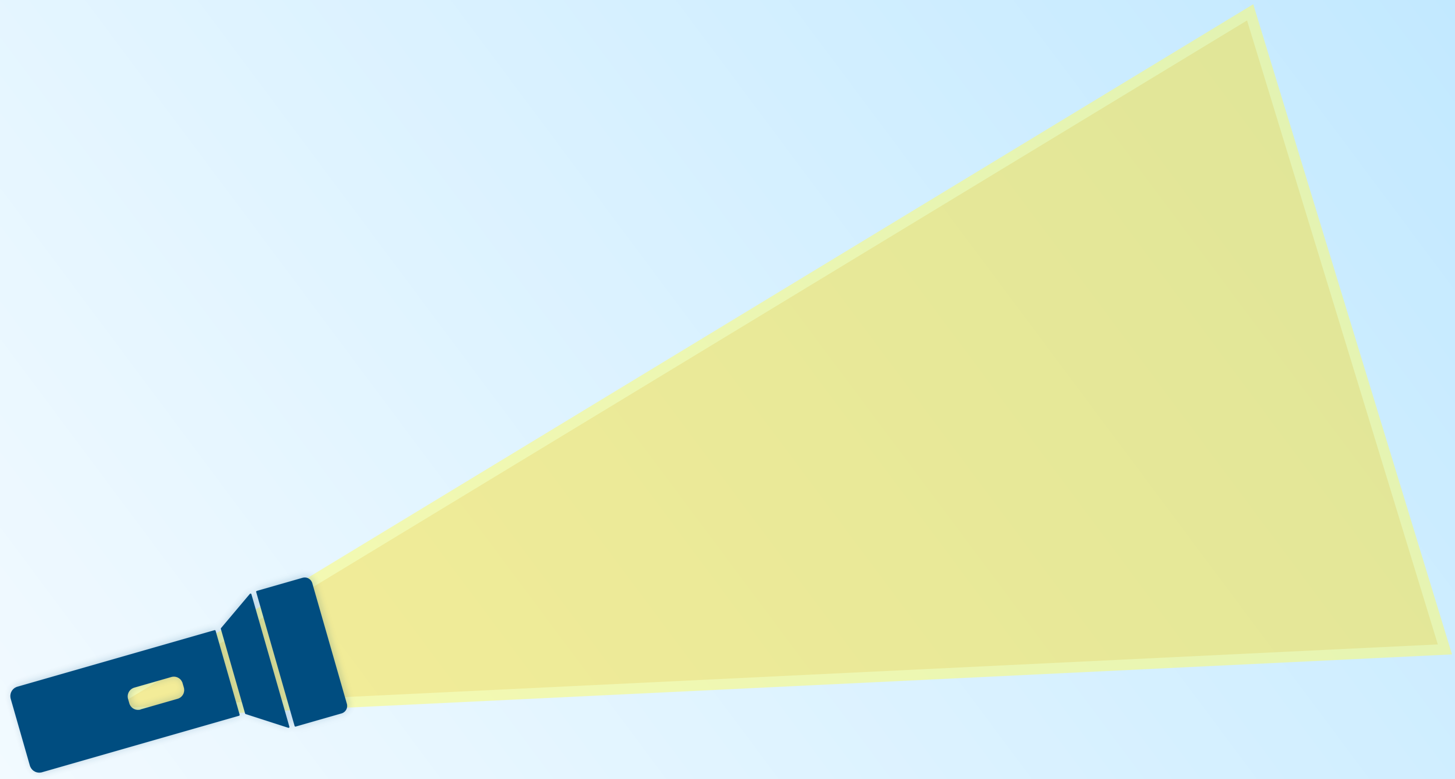

Graham+20, Graham+23, Ashton+21

Predictions on **binary parameters** and **comparison** to **observations**

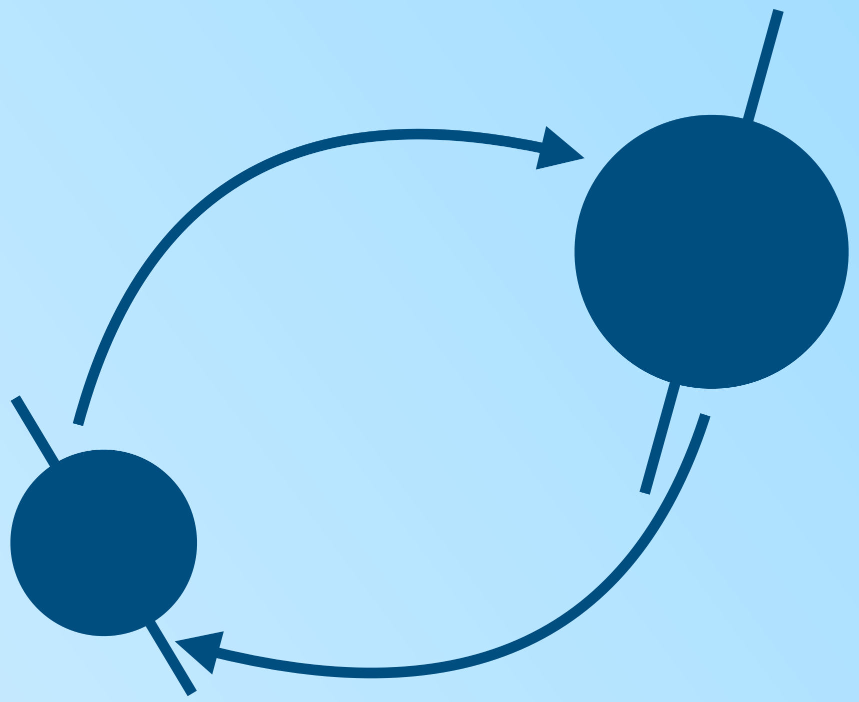

McKernan+20, Romero-Shaw+21, Gayathri+21, Karathanasis+22, …

Investigation of **spatial correlation** with potential hosts

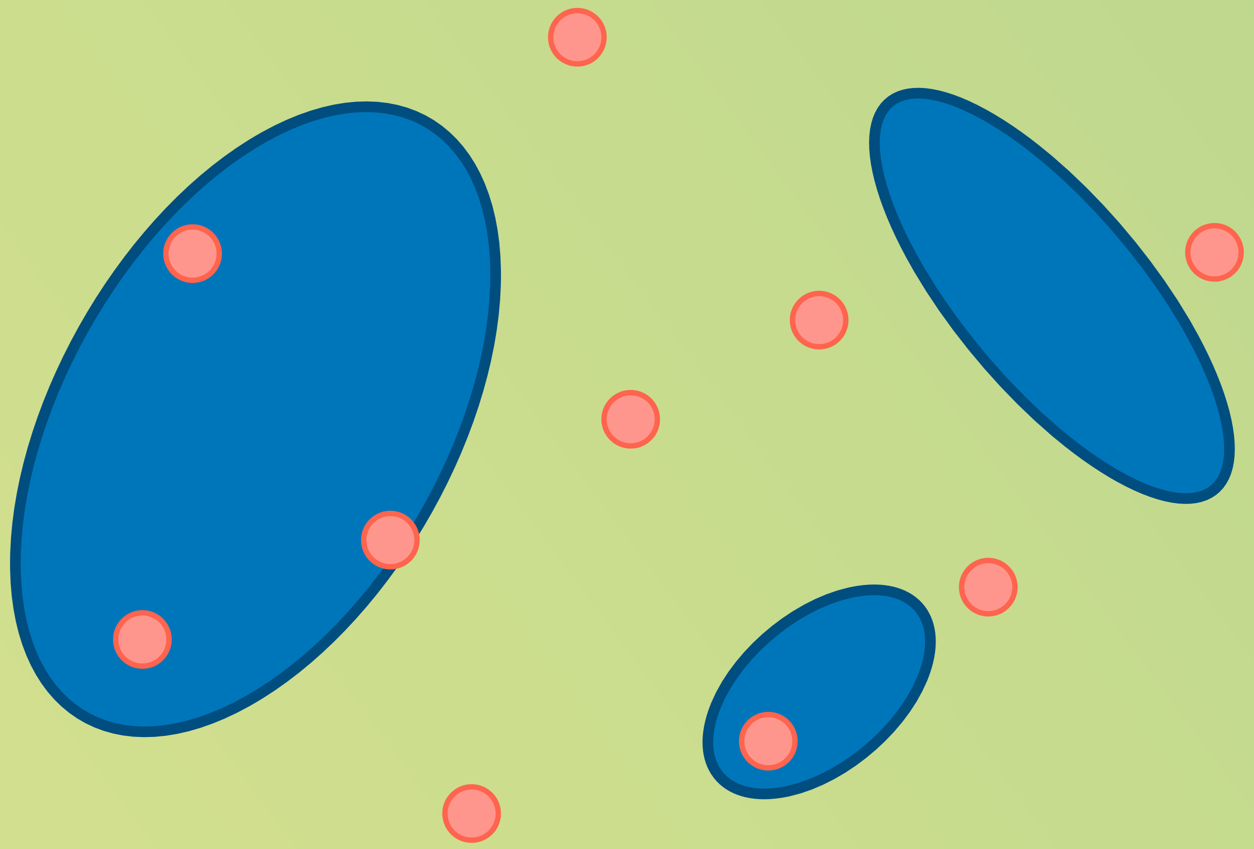

Bartos+17, Corley+19, NV+22, NV+23

$$f_{\mathrm{AGN}} = ?$$

Fraction of detected BBH mergers that happened in an AGN

Why focusing on AGN?

CTIVE ALACTIC UCLEI

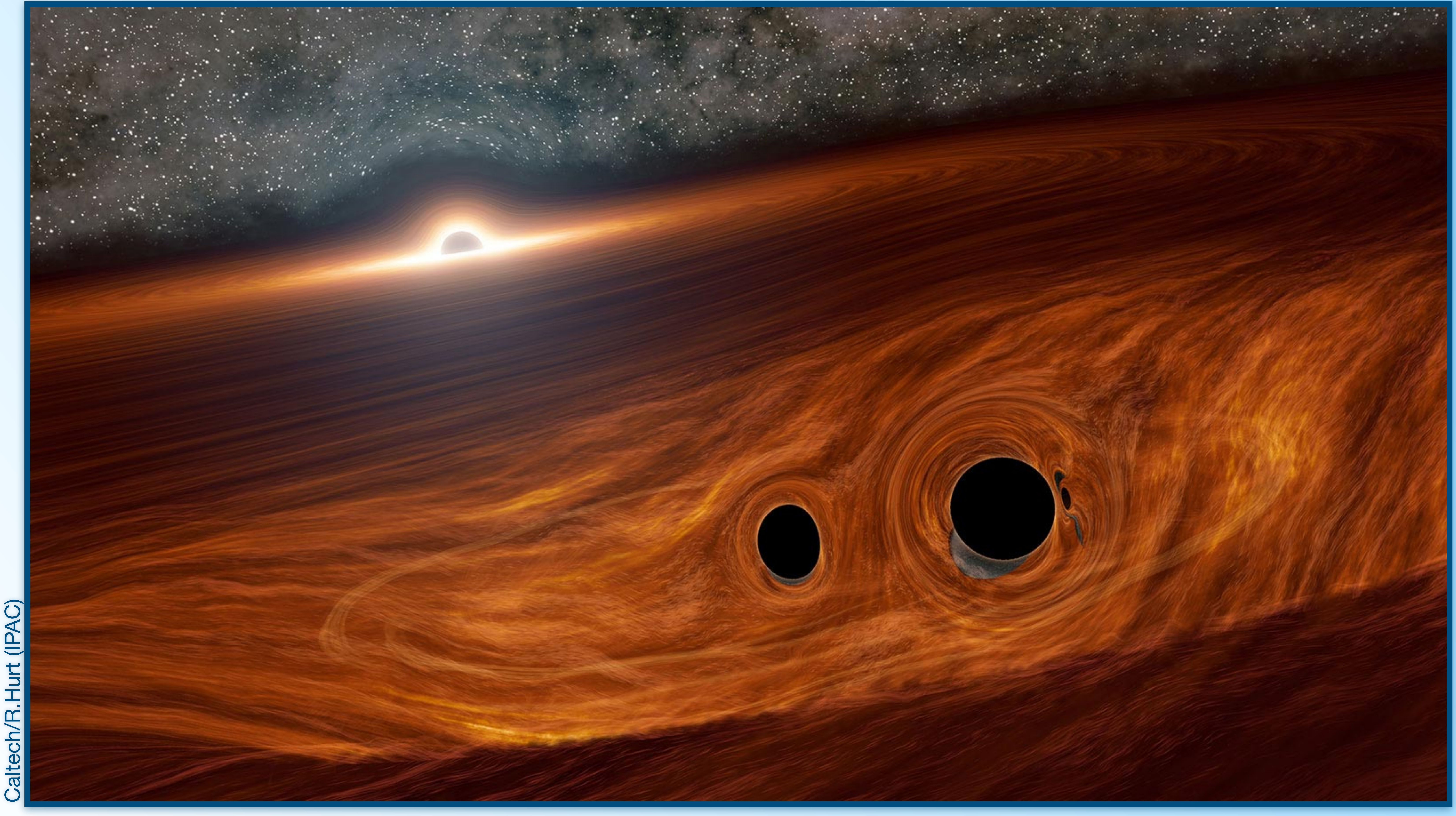

Caltech/R.Hurt (IPAC)

McKernan+11, McKernan+12, Bellovary+16, Tagawa+20

Why focusing on AGN?

CTIVE ALACTIC UCLEI

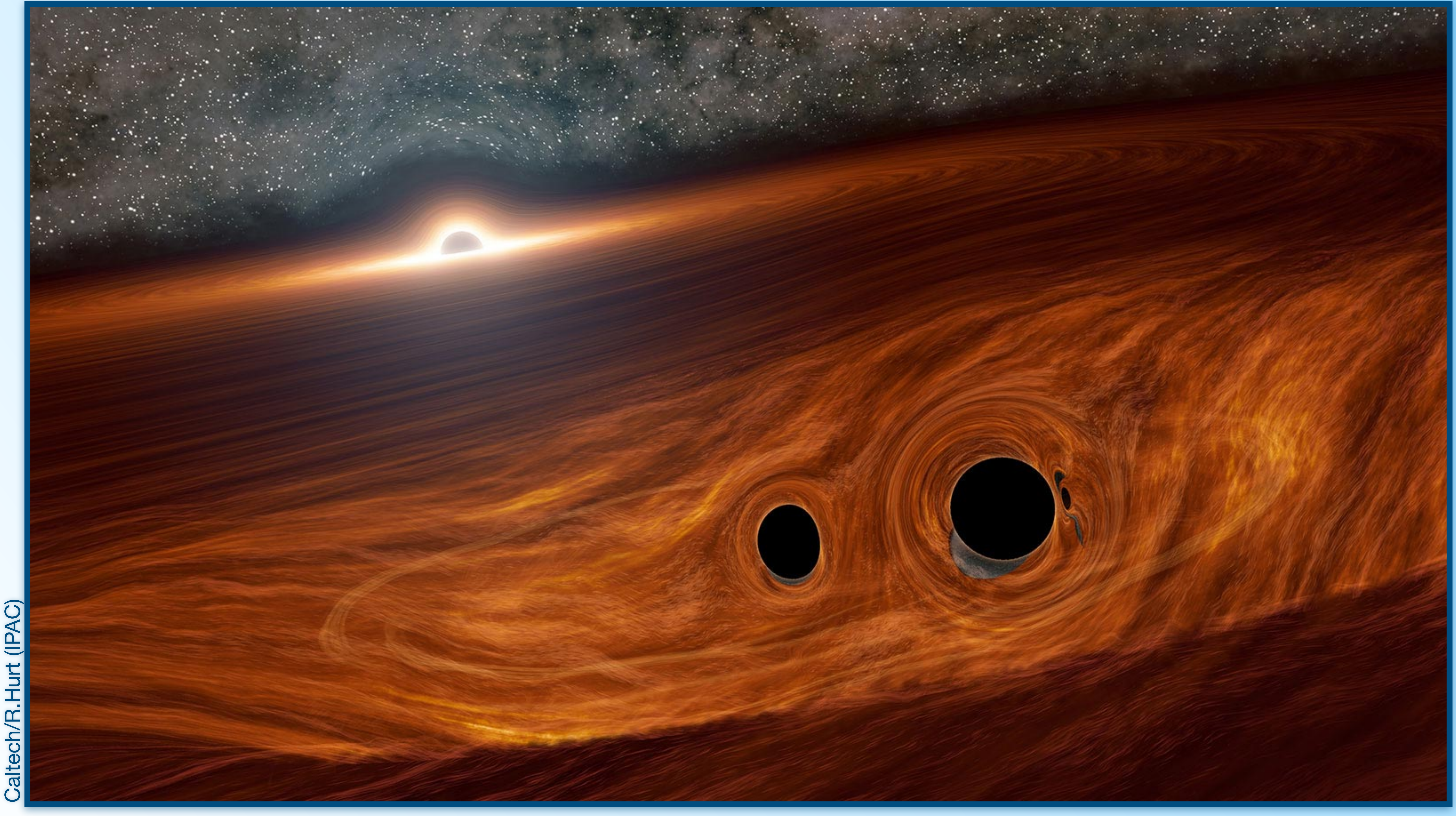

Caltech/R.Hurt (IPAC)

- Dense dynamical environments
  High chance of binary formation

McKernan+11, McKernan+12,
Bellovary+16, Tagawa+20

Why focusing on AGN?

C T I V E | A L A C T I C | U C L E I

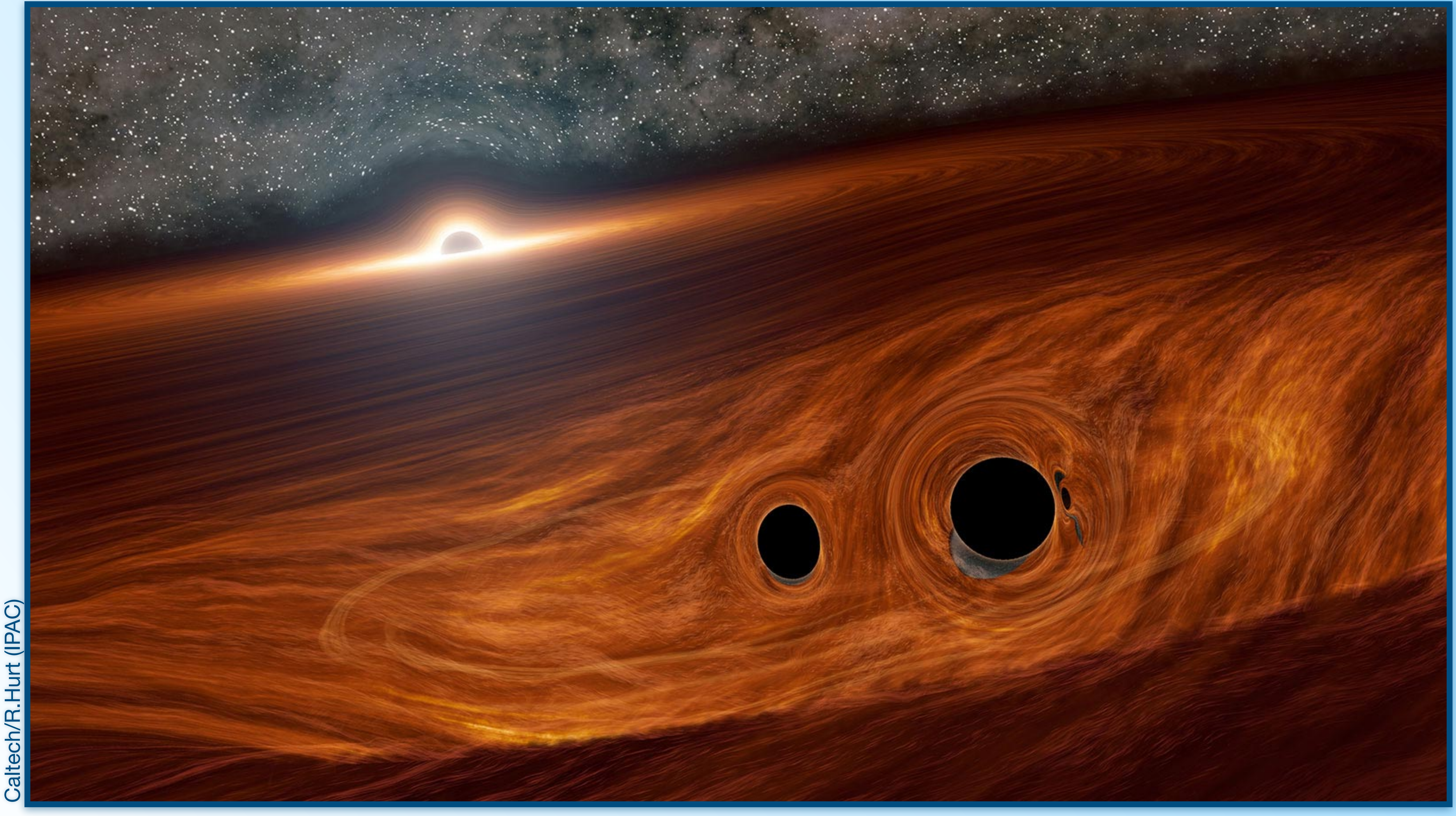

Caltech/R.Hurt (IPAC)

- Dense dynamical environments
  High chance of binary formation

- Deep gravitational potential
  Possibility of retain kicked remnants

McKernan+11, McKernan+12, Bellovary+16, Tagawa+20

Why focusing on AGN?

CTIVE ALACTIC UCLEI

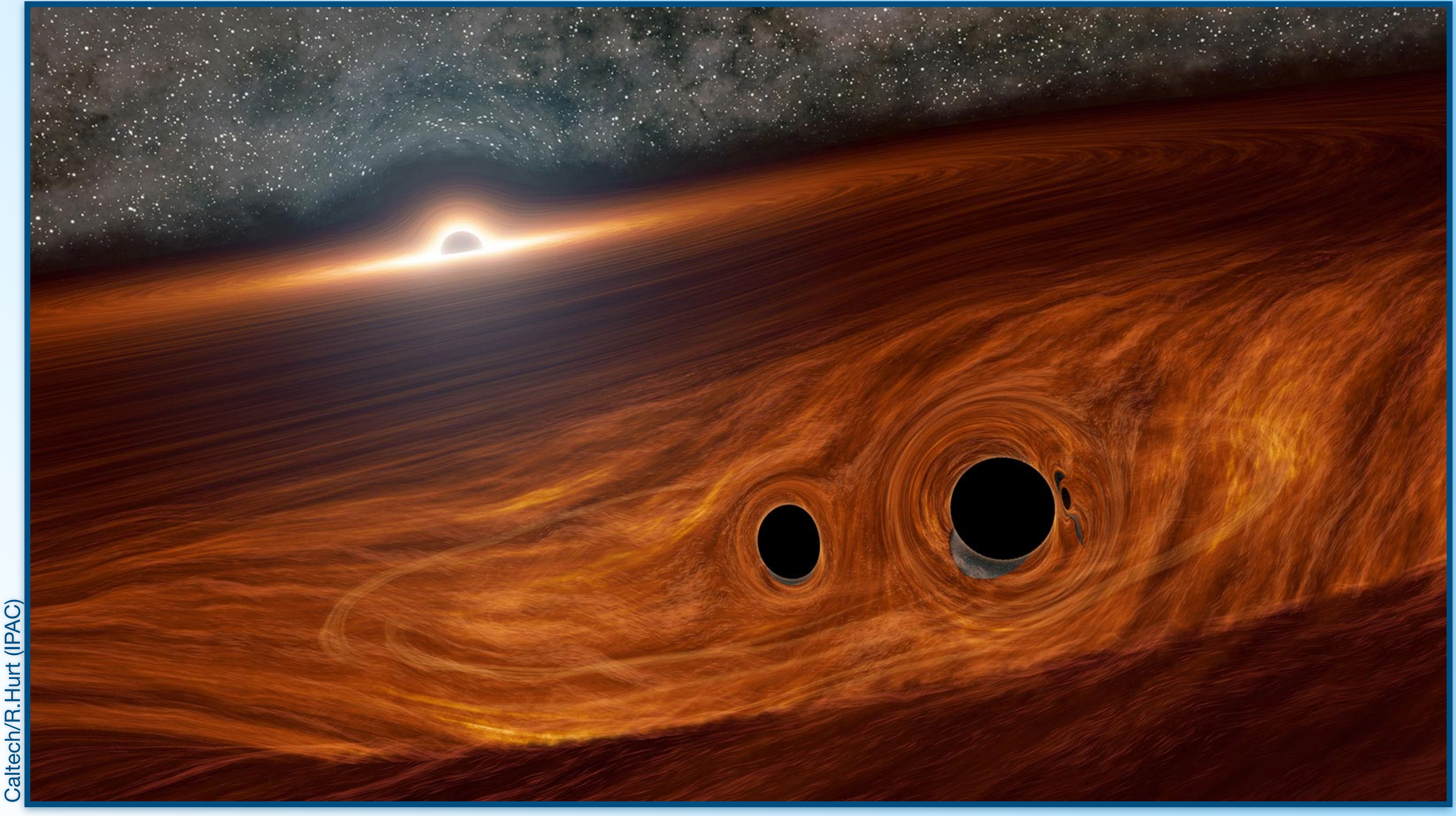

Caltech/R.Hurt (IPAC)

- Dense dynamical environments
  High chance of binary formation
- Deep gravitational potential
  Possibility of retain kicked remnants
- Migration (traps)
  Gathering many compact objects in the same region

McKernan+11, McKernan+12, Bellovary+16, Tagawa+20

If only it was this easy…

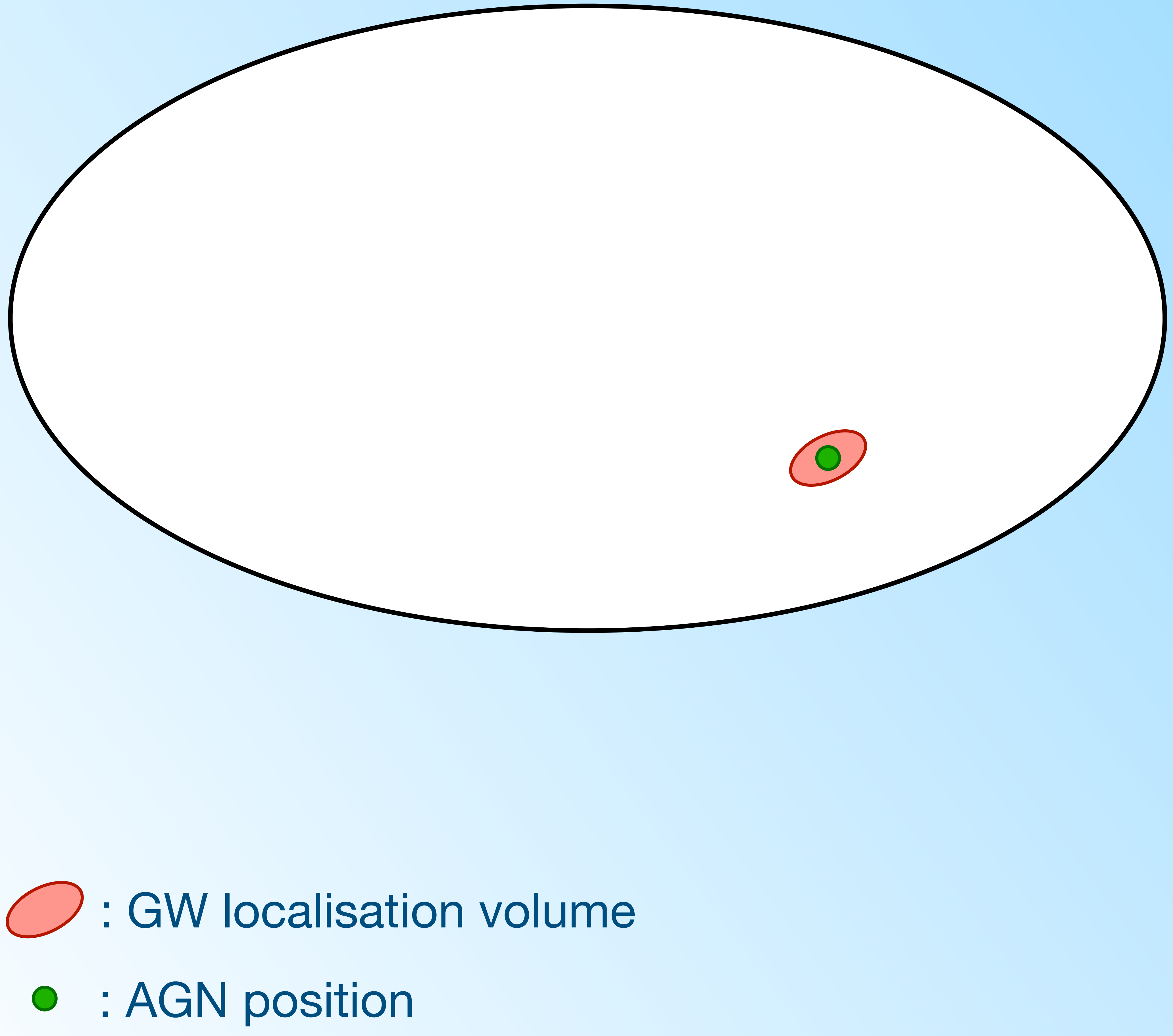

If only it was this easy…

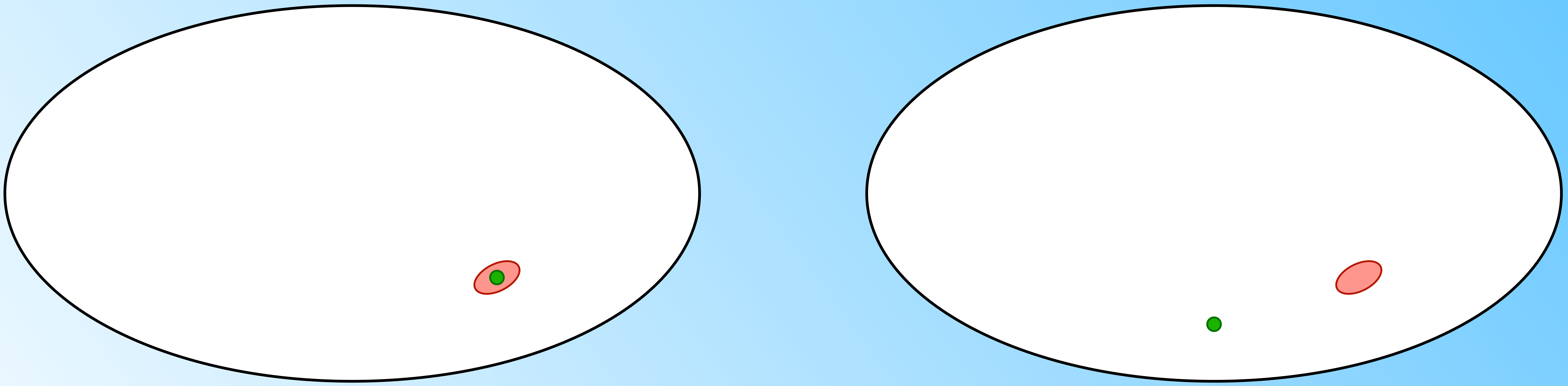

: GW localisation volume

: AGN position

If only it was this easy…

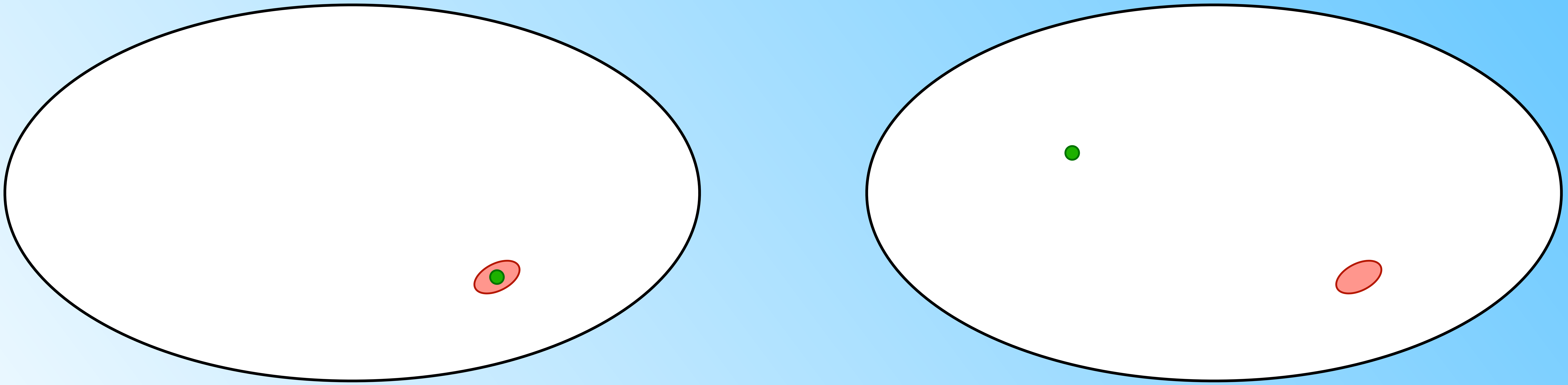

: GW localisation volume

: AGN position

If only it was this easy…

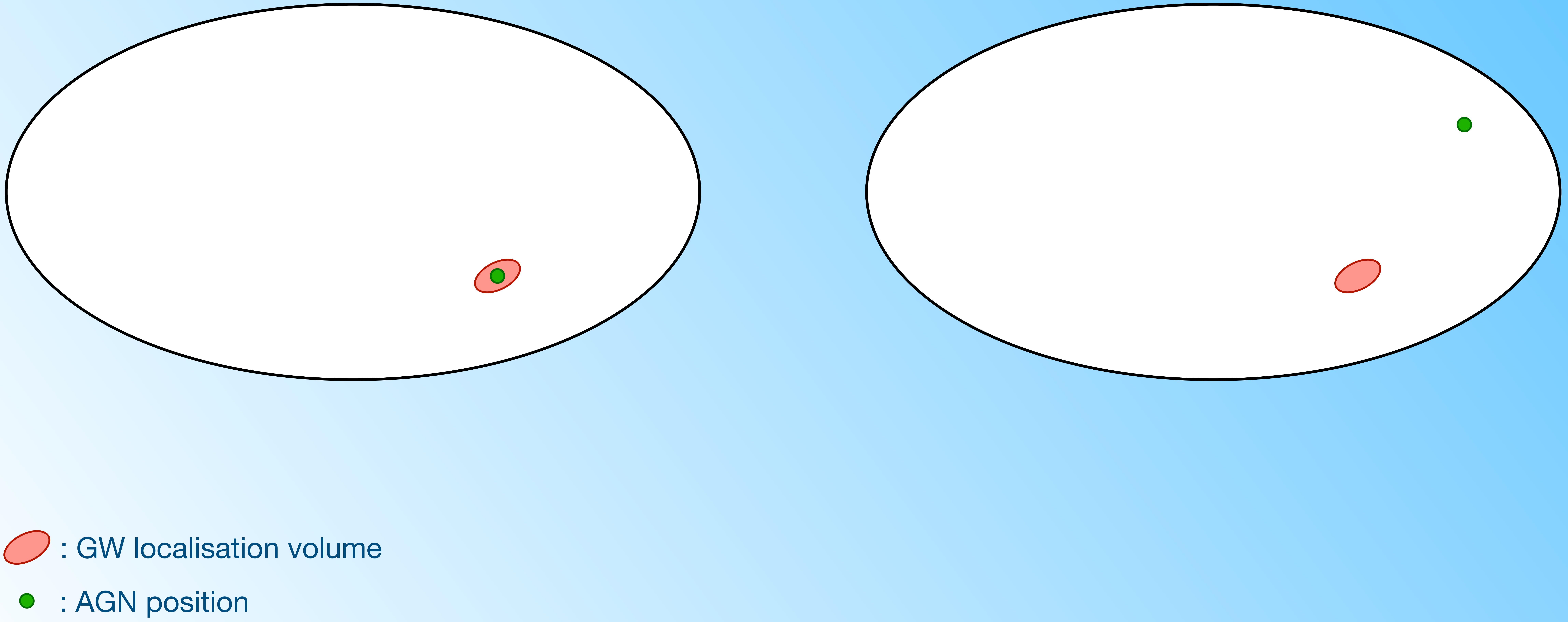

If only it was this easy…

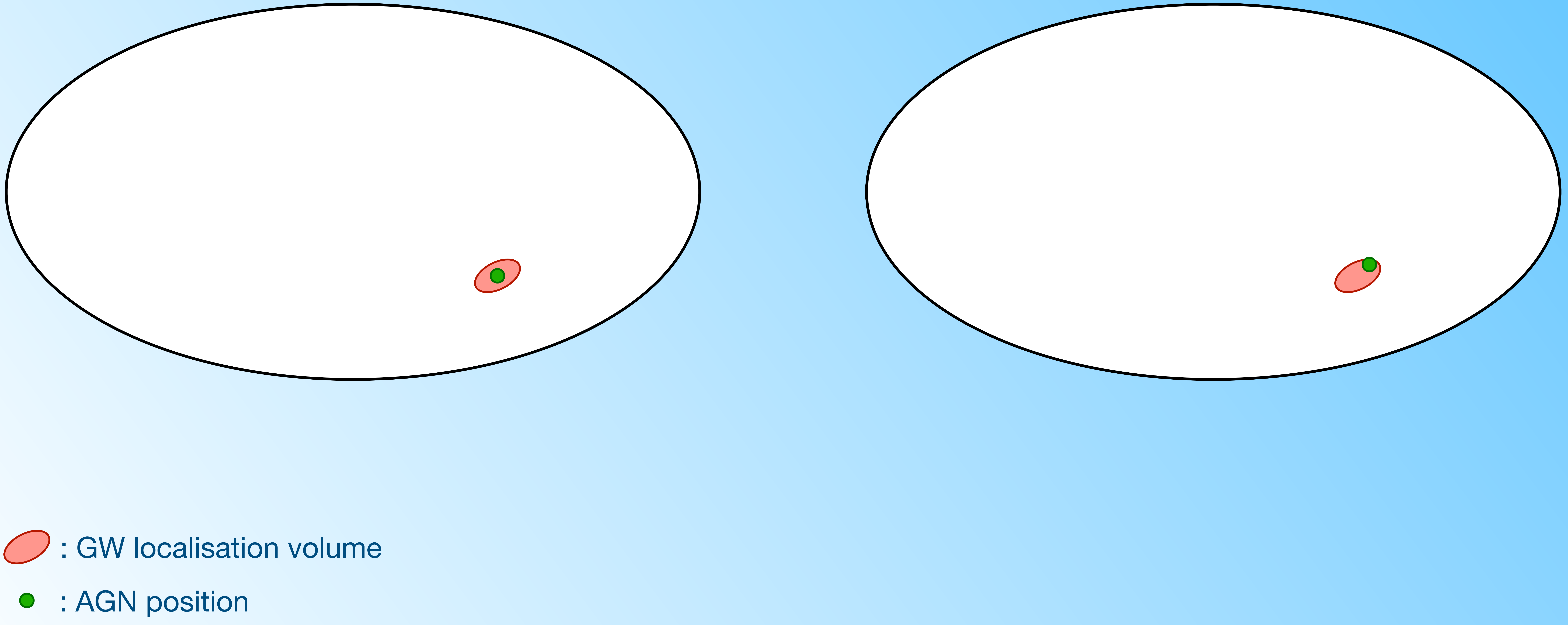

If only it was this easy…

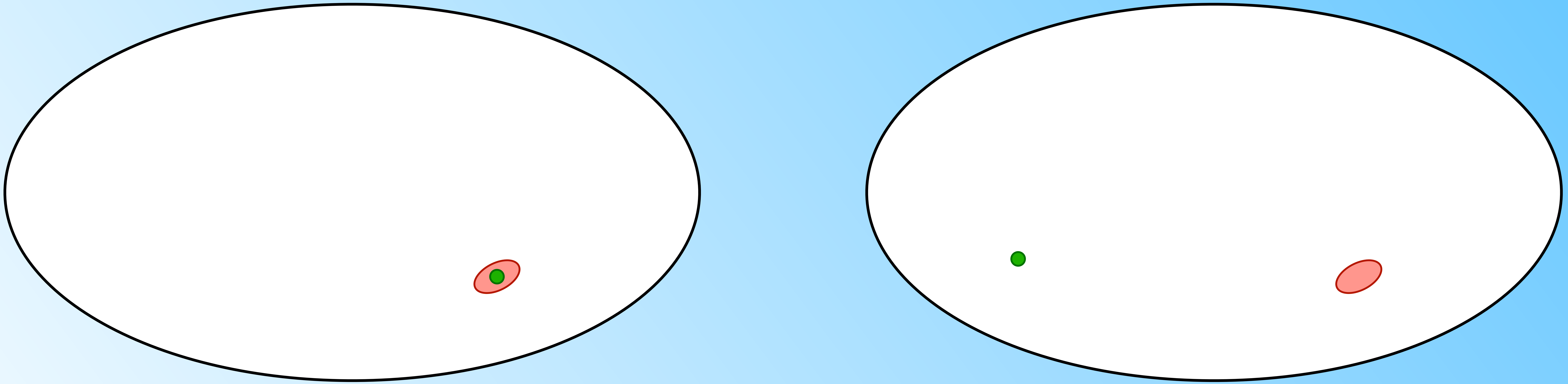

The real picture

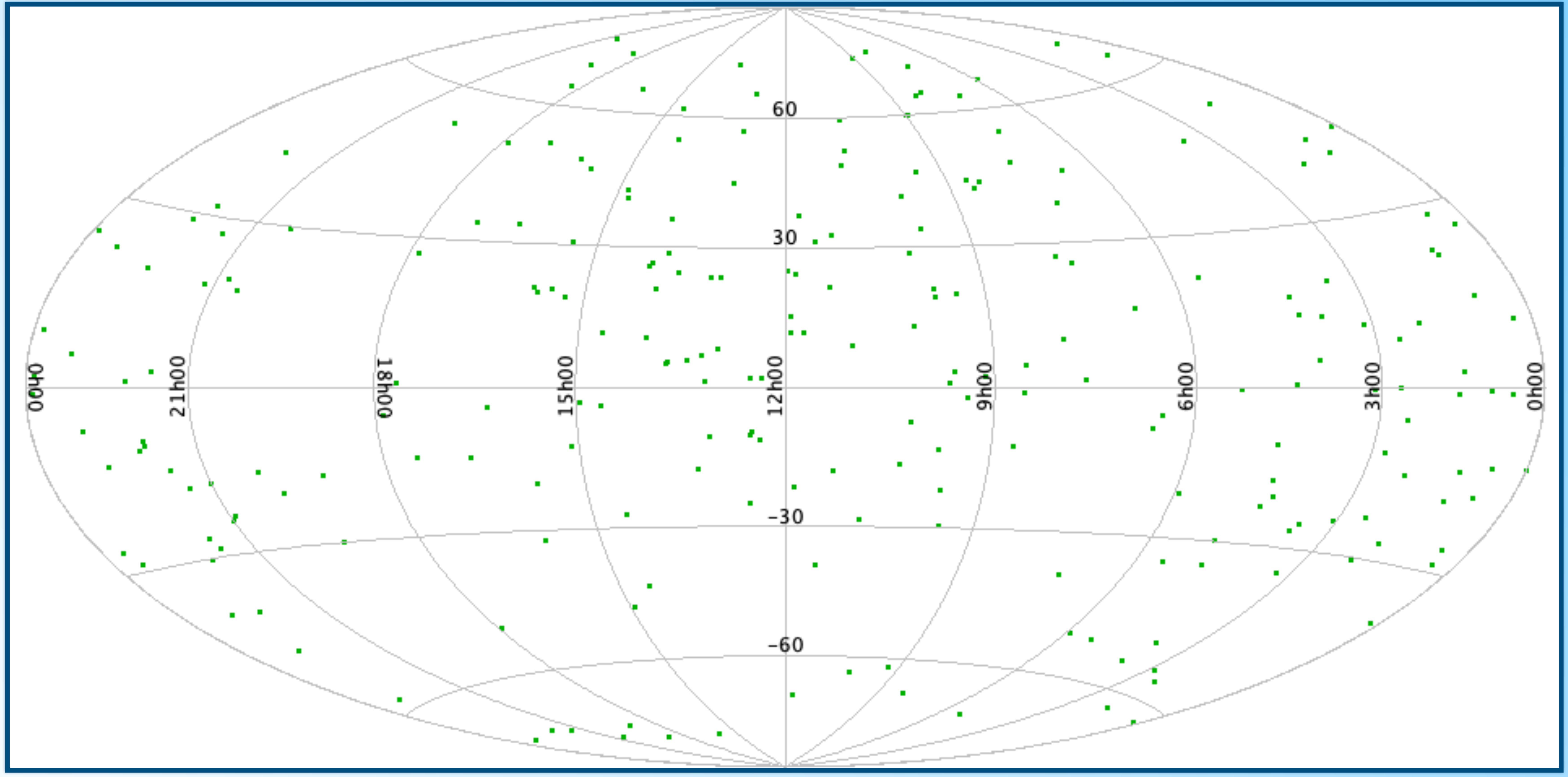

● $L_{\rm bol} \geq 10^{46}$ erg s−1
242 AGN

AGN from unWISE (Schlafly+19) with spectroscopic redshift from Milliquas v7.7b (Flesch21)

The real picture

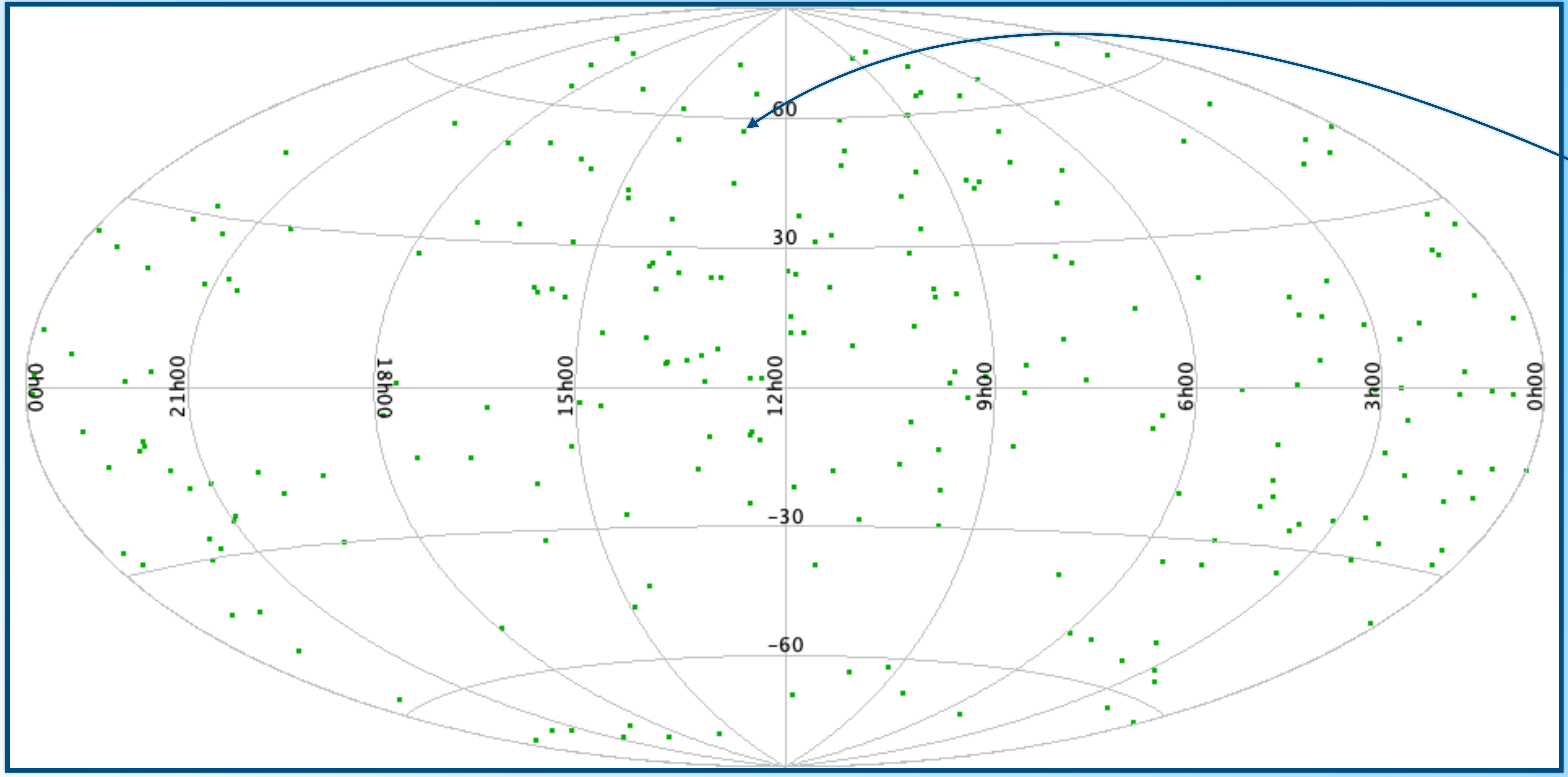

UGC 8058
Nearest known Quasar

● $L_{bol} \geq 10^{46}$ erg s−1
242 AGN

AGN from unWISE (Schlafly+19) with spectroscopic redshift from Milliquas v7.7b (Flesch21)

The real picture

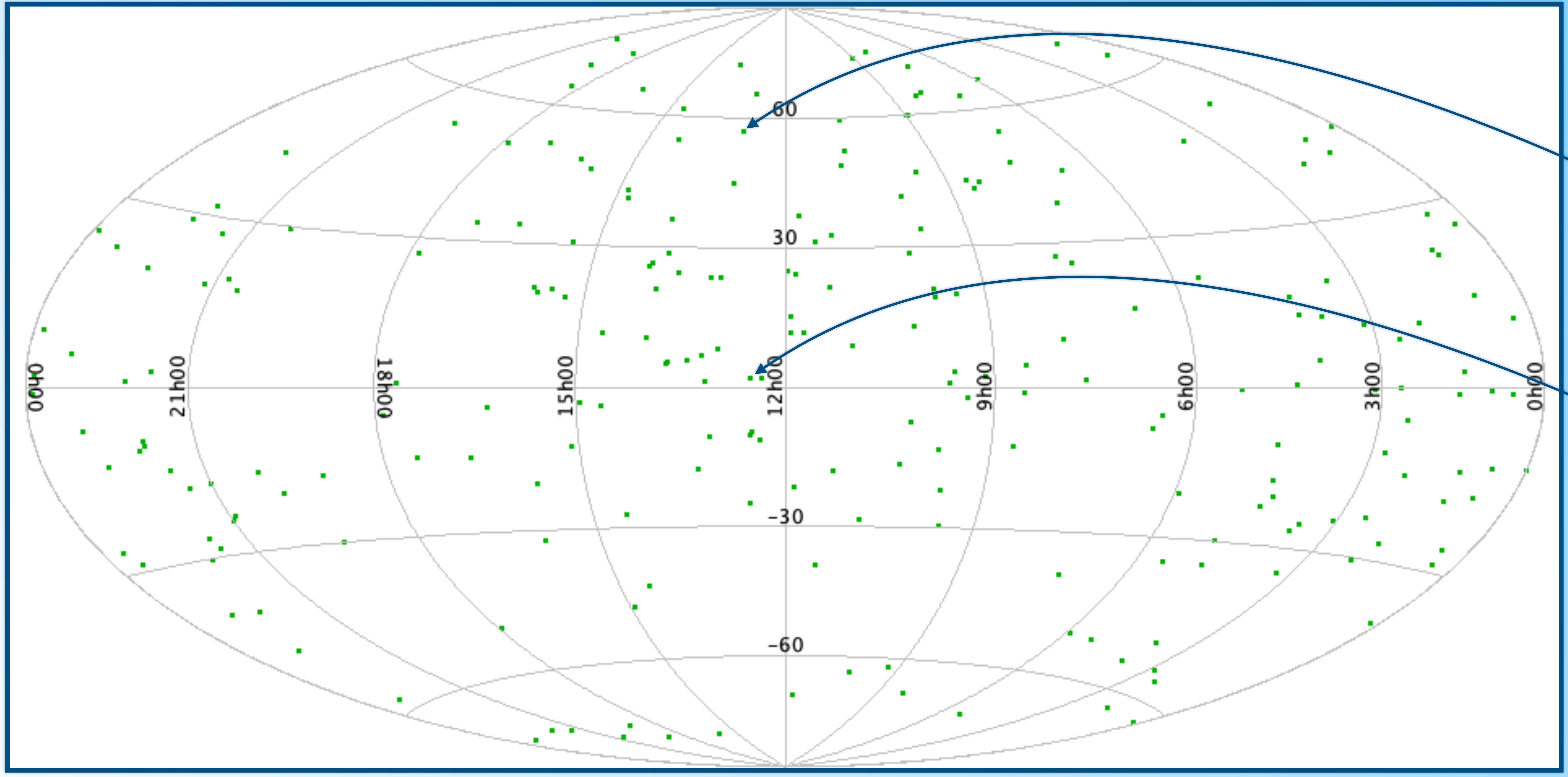

UGC 8058
Nearest known Quasar

3C 273
First Quasar ever to be identified

● $L_{\rm bol} \geq 10^{46}\,{\rm erg\,s}^{-1}$
242 AGN

AGN from unWISE (Schlafly+19) with spectroscopic redshift from Milliquas v7.7b (Flesch21)

The real picture

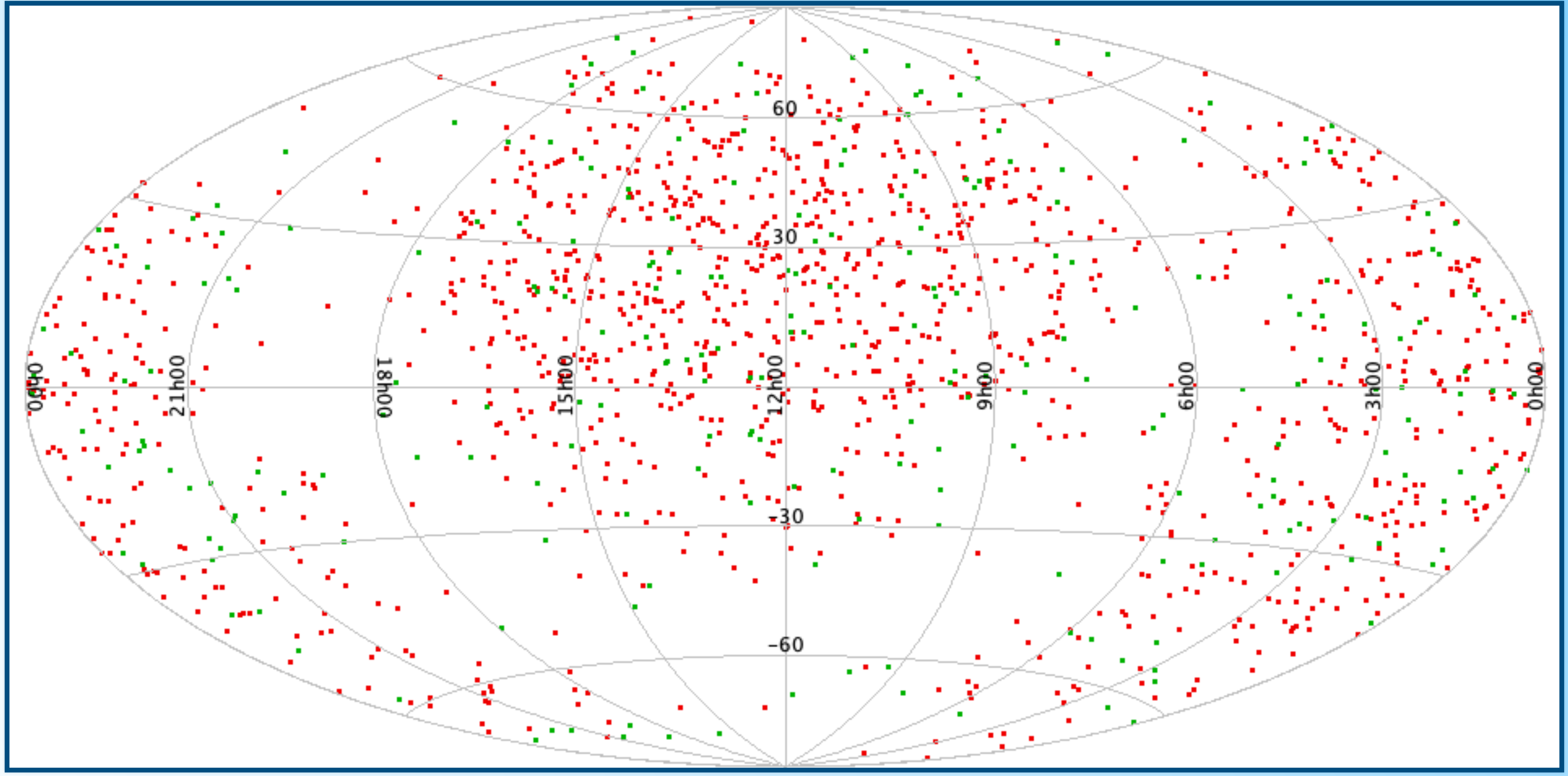

● $L_{bol} \geq 10^{45.5}$ erg s^{-1}
1,412 AGN

● $L_{bol} \geq 10^{46}$ erg s^{-1}
242 AGN

AGN from unWISE (Schlafly+19) with spectroscopic redshift from Milliquas v7.7b (Flesch21)

The real picture

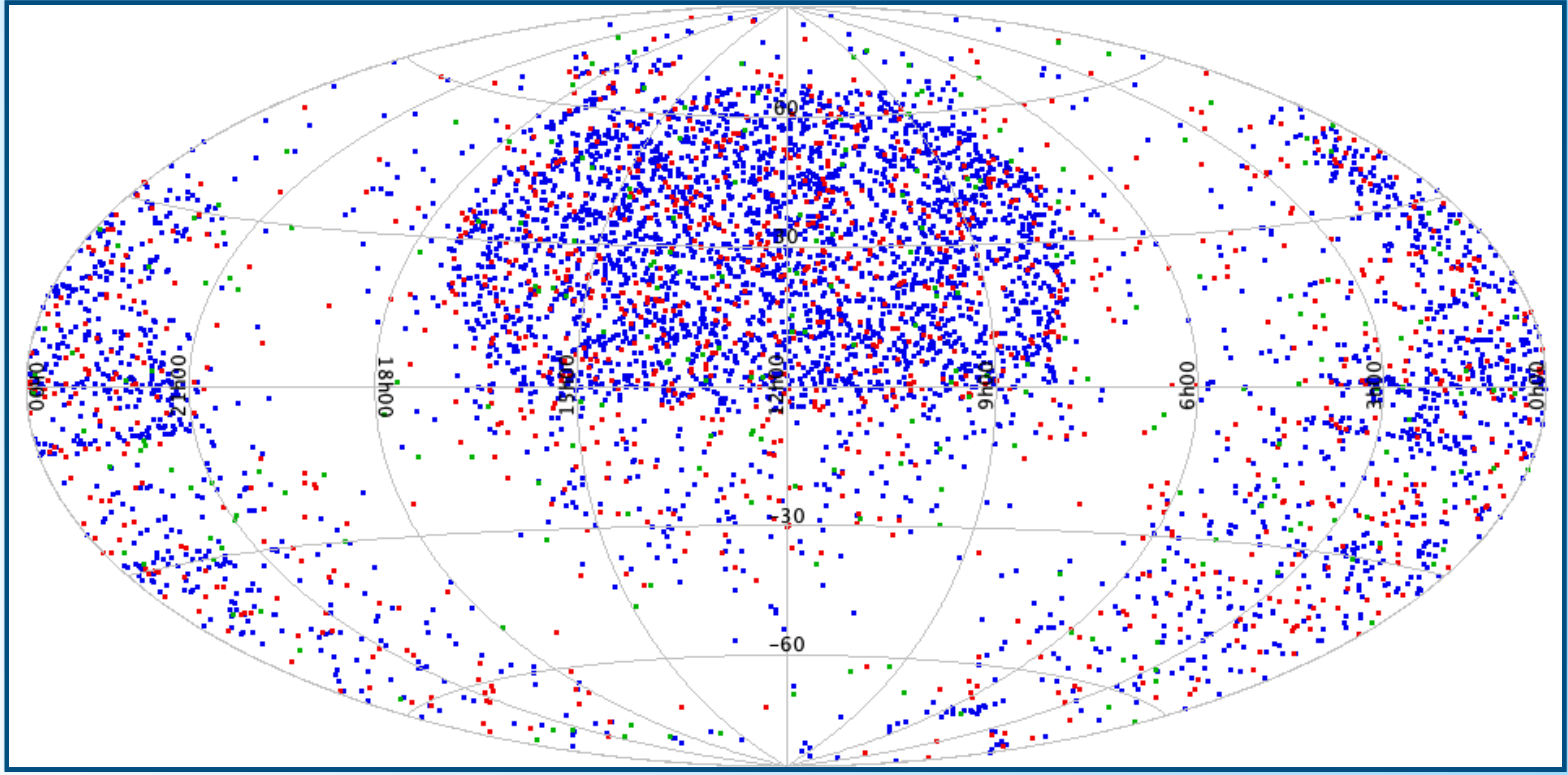

● $L_{bol} \geq 10^{45}$ erg s^{-1} 5,791 AGN

● $L_{bol} \geq 10^{45.5}$ erg s^{-1} 1,412 AGN

● $L_{bol} \geq 10^{46}$ erg s^{-1} 242 AGN

AGN from unWISE (Schlafly+19) with spectroscopic redshift from Milliquas v7.7b (Flesch21)

The real picture

GW skymaps for the 30 BBHs from O1, O2, and O3 with $z \leq 0.3$ with 90% credibility

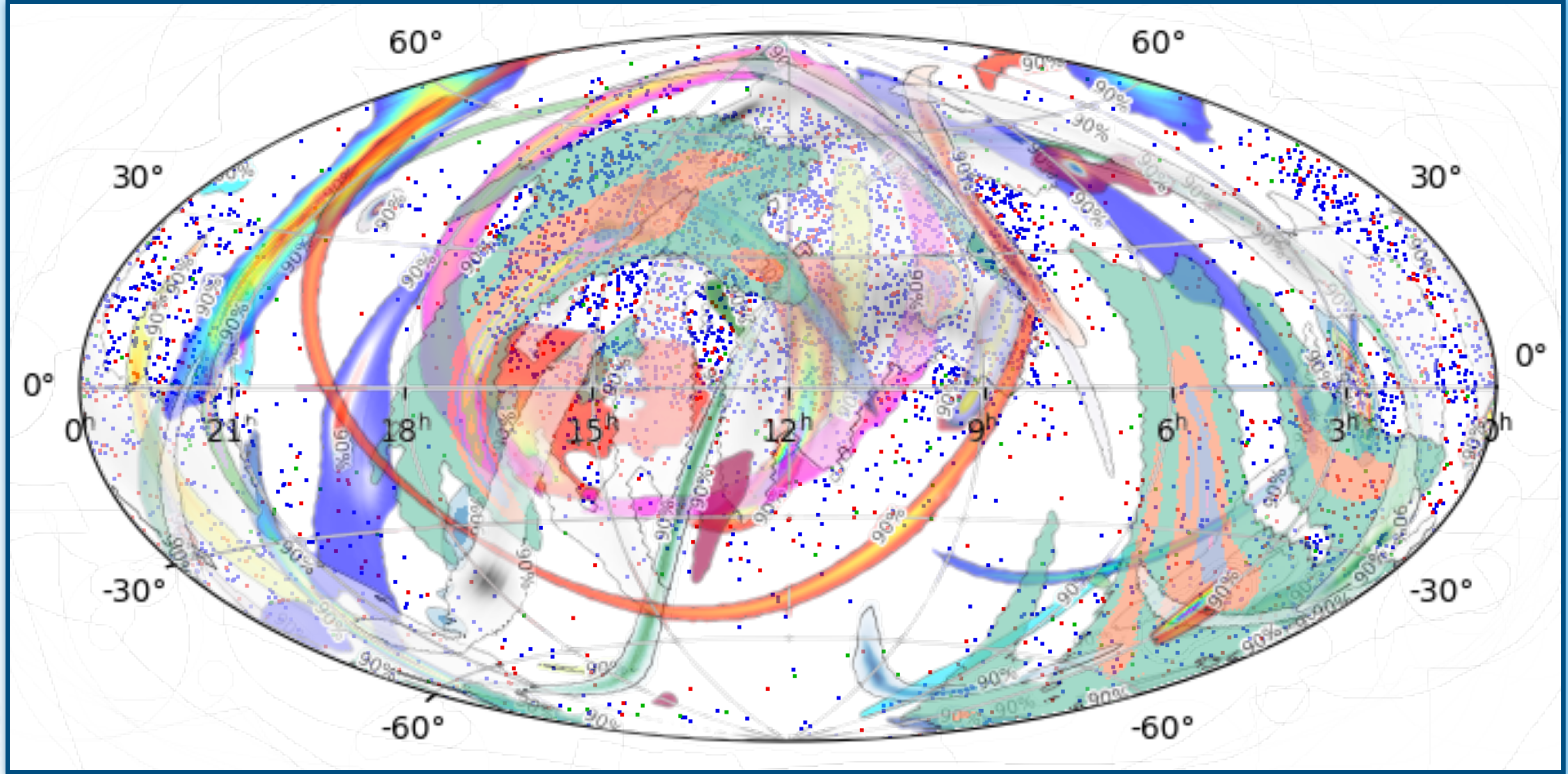

NV+23

● $L_{\rm bol} \geq 10^{45}\,{\rm erg\,s^{-1}}$ 5,791 AGN

● $L_{\rm bol} \geq 10^{45.5}\,{\rm erg\,s^{-1}}$ 1,412 AGN

● $L_{\rm bol} \geq 10^{46}\,{\rm erg\,s^{-1}}$ 242 AGN

AGN from unWISE (Schlafly+19) with spectroscopic redshift from Milliquas v7.7b (Flesch21)

The real picture

GW skymaps for the 30 BBHs from O1, O2, and O3 with $z \leq 0.3$ with 90% credibility

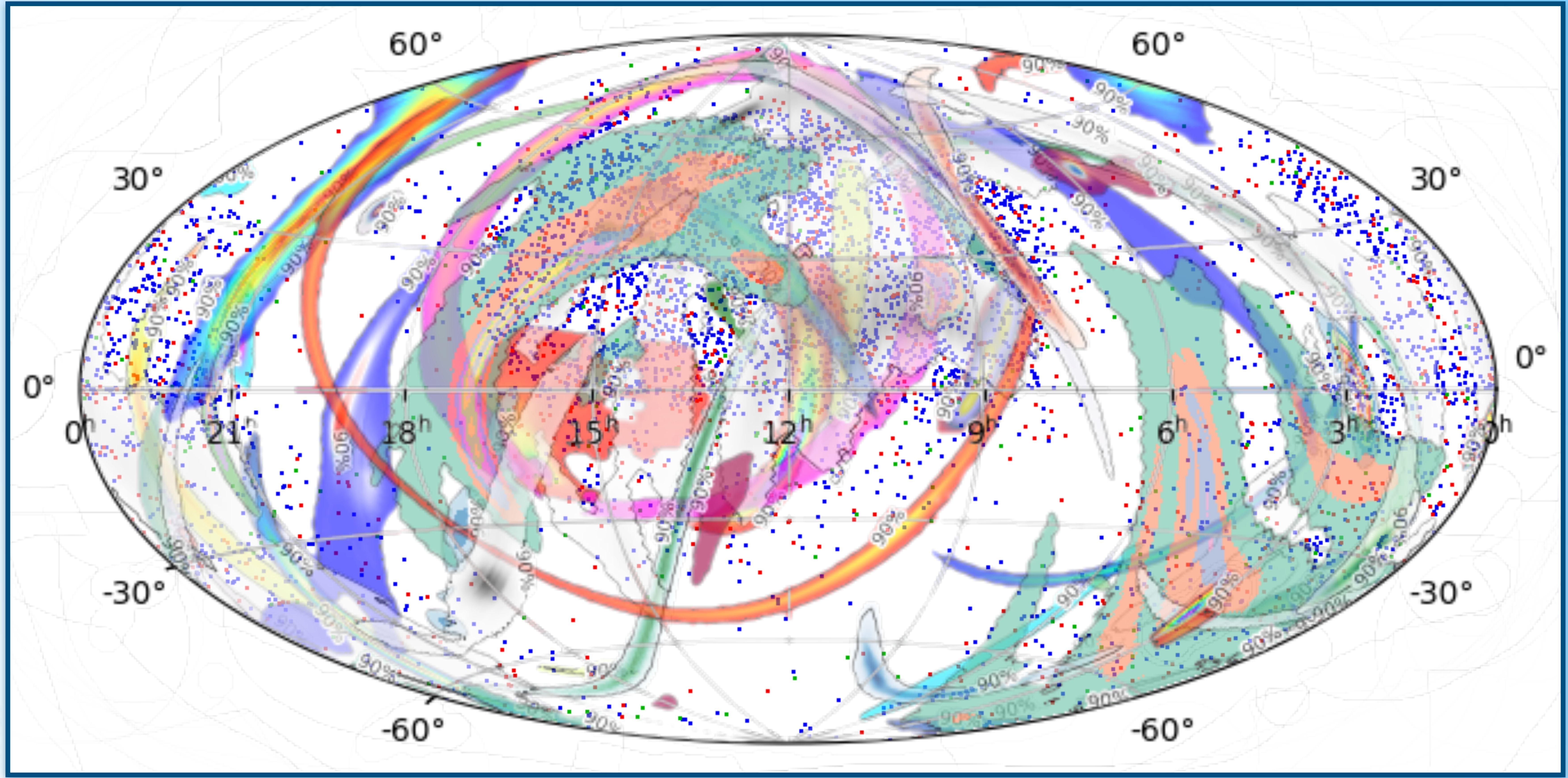

NV+23

- More AGN
  Bad

● $L_{\rm bol} \geq 10^{45}\,{\rm erg\,s^{-1}}$ 5,791 AGN

● $L_{\rm bol} \geq 10^{45.5}\,{\rm erg\,s^{-1}}$ 1,412 AGN

● $L_{\rm bol} \geq 10^{46}\,{\rm erg\,s^{-1}}$ 242 AGN

AGN from unWISE (Schlafly+19) with spectroscopic redshift from Milliquas v7.7b (Flesch21)

The real picture

GW skymaps for the 30 BBHs from O1, O2, and O3 with $z \leq 0.3$ with 90% credibility

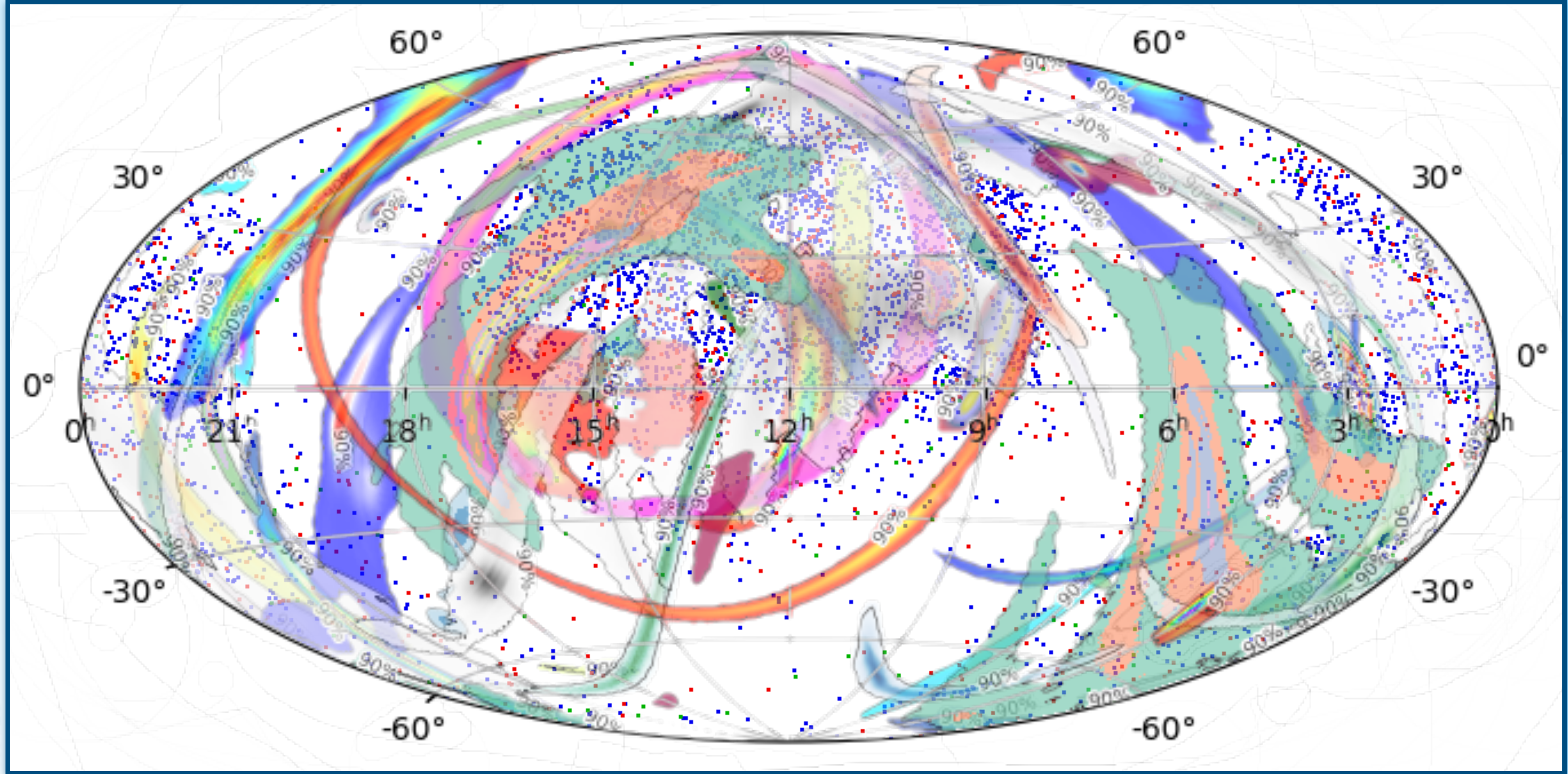

NV+23

- $L_{\rm bol} \geq 10^{45}$ erg s^{-1} — 5,791 AGN
- $L_{\rm bol} \geq 10^{45.5}$ erg s^{-1} — 1,412 AGN
- $L_{\rm bol} \geq 10^{46}$ erg s^{-1} — 242 AGN

AGN from unWISE (Schlafly+19) with spectroscopic redshift from Milliquas v7.7b (Flesch21)

- More AGN
  Bad
- More detected BBH mergers
  Good

The real picture

GW skymaps for the **30 BBHs** from O1, O2, and O3 with $z \leq 0.3$ with 90% credibility

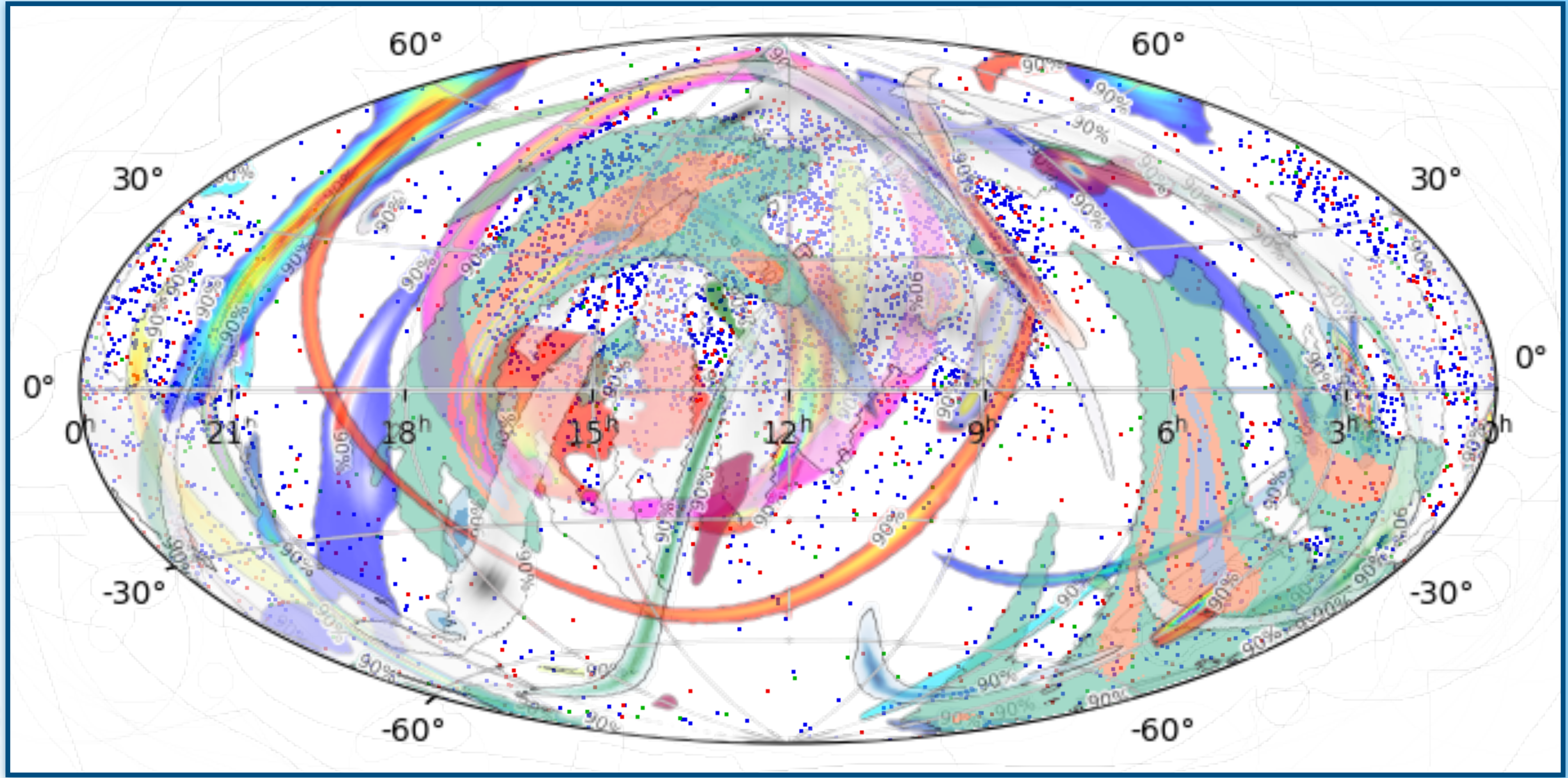

- More AGN
  Bad
- More detected BBH mergers
  Good
- Large localisation volumes
  Bad

● $L_{bol} \geq 10^{45}$ erg s^{-1} 5,791 AGN

● $L_{bol} \geq 10^{45.5}$ erg s^{-1} 1,412 AGN

● $L_{bol} \geq 10^{46}$ erg s^{-1} 242 AGN

AGN from unWISE (Schlafly+19) with spectroscopic redshift from Milliquas v7.7b (Flesch21)

The real picture

GW skymaps for the 30 BBHs from O1, O2, and O3 with $z \leq 0.3$ with 90% credibility

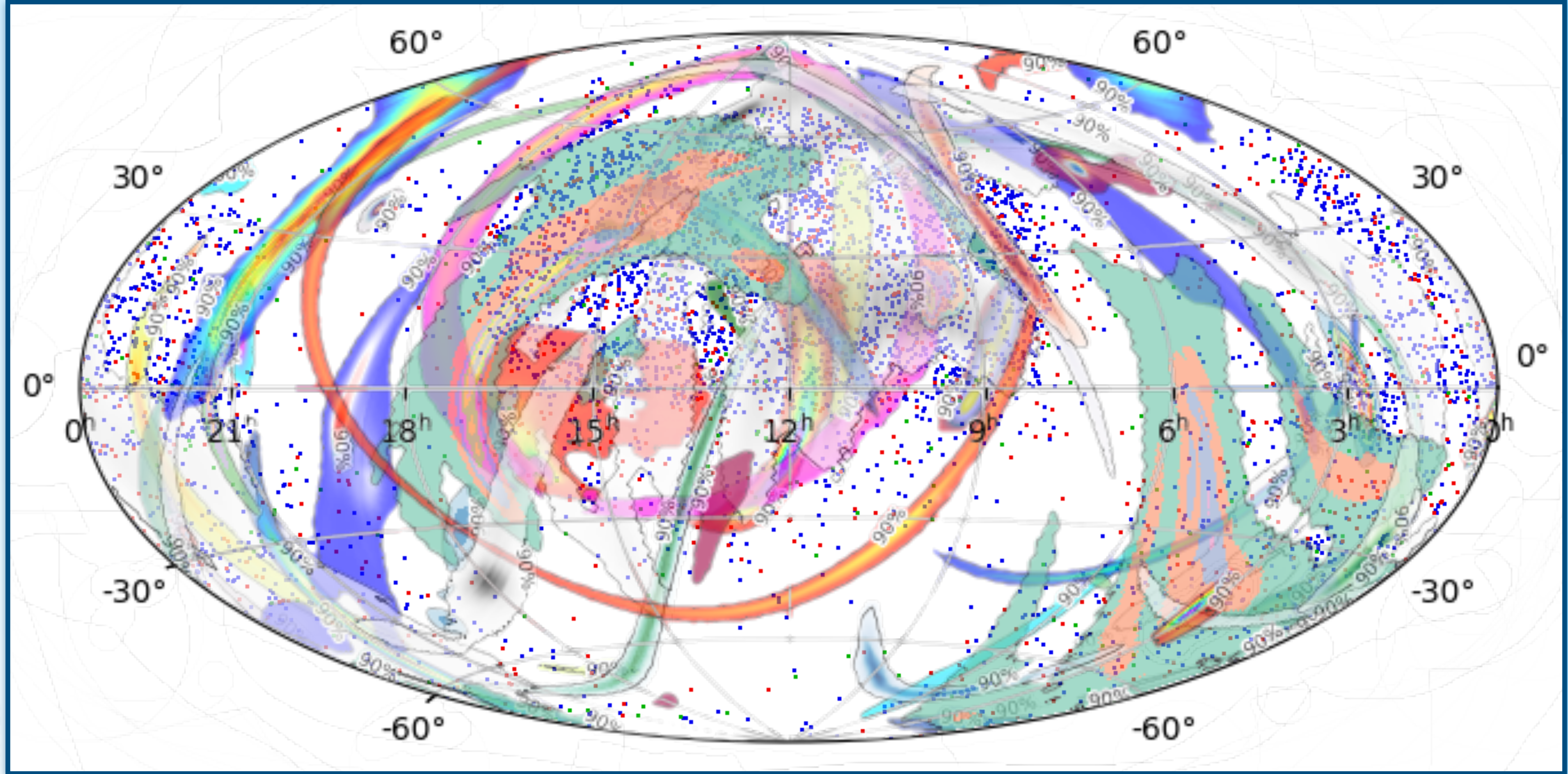

NV+23

$L_{bol} \geq 10^{45}$ erg s^{-1} — 5,791 AGN

$L_{bol} \geq 10^{45.5}$ erg s^{-1} — 1,412 AGN

$L_{bol} \geq 10^{46}$ erg s^{-1} — 242 AGN

AGN from unWISE (Schlafly+19) with spectroscopic redshift from Milliquas v7.7b (Flesch21)

- More AGN
  Bad
- More detected BBH mergers
  Good
- Large localisation volumes
  Bad
- Incomplete AGN catalogues
  Bad

Our method

$$\mathcal{L}\left(f_{\mathrm{AGN}}\right) = \prod_{i=1}^{N_{\mathrm{GW}}} \left[c \cdot 0.9 \cdot f_{\mathrm{AGN}} \cdot \mathcal{S}_i + \left(1 - c \cdot 0.90 \cdot f_{\mathrm{AGN}}\right) \mathcal{B}_i\right]$$

$$\mathcal{S}_i = \frac{\sum_{j=1}^{N_{\mathrm{V90}_i}} p_j}{n_{\mathrm{AGN}} \mathrm{V90}_i}$$

$$\mathcal{B}_i = \frac{0.9}{\mathrm{V90}_i}$$

Our method

Multiple detected BBH mergers ✓

$$\mathcal{L}\left(f_{\mathrm{AGN}}\right) = \prod_{i=1}^{N_{\mathrm{GW}}} \left[c \cdot 0.9 \cdot f_{\mathrm{AGN}} \cdot \mathcal{S}_i + \left(1 - c \cdot 0.90 \cdot f_{\mathrm{AGN}}\right) \mathcal{B}_i\right]$$

$$\mathcal{S}_i = \frac{\sum_{j=1}^{N_{\mathrm{V90}_i}} p_j}{n_{\mathrm{AGN}} \mathrm{V90}_i}$$

$$\mathcal{B}_i = \frac{0.9}{\mathrm{V90}_i}$$

Our method

Multiple detected BBH mergers ✓

$$\mathcal{L}\left(f_{\mathrm{AGN}}\right) = \prod_{i=1}^{N_{\mathrm{GW}}} \left[c \cdot 0.9 \cdot f_{\mathrm{AGN}} \cdot \mathcal{S}_i + \left(1 - c \cdot 0.90 \cdot f_{\mathrm{AGN}}\right) \mathcal{B}_i\right]$$

$$\mathcal{S}_i = \frac{\sum_{j=1}^{N_{\mathrm{V90}_i}} p_j}{n_{\mathrm{AGN}} \mathrm{V90}_i}$$

$$\mathcal{B}_i = \frac{0.9}{\mathrm{V90}_i}$$

Multiple AGN ✓

Our method

Multiple detected BBH mergers ✓

$$\mathcal{L}(f_{\mathrm{AGN}}) = \prod_{i=1}^{N_{\mathrm{GW}}} \left[c \cdot 0.9 \cdot f_{\mathrm{AGN}} \cdot \mathcal{S}_i + (1 - c \cdot 0.90 \cdot f_{\mathrm{AGN}})\, \mathcal{B}_i\right]$$

$$\mathcal{S}_i = \frac{\sum_{j=1}^{N_{\mathrm{V90}_i}} p_j}{n_{\mathrm{AGN}} \mathrm{V90}_i}$$

$$\mathcal{B}_i = \frac{0.9}{\mathrm{V90}_i}$$

Number of AGN within localisation volumes ✓

Multiple AGN ✓

Our method

Multiple detected BBH mergers ✓

$$\mathcal{L}\left(f_{\mathrm{AGN}}\right) = \prod_{i=1}^{N_{\mathrm{GW}}} \left[c \cdot 0.9 \cdot f_{\mathrm{AGN}} \cdot \mathcal{S}_i + \left(1 - c \cdot 0.90 \cdot f_{\mathrm{AGN}}\right) \mathcal{B}_i\right]$$

$$\mathcal{S}_i = \frac{\sum_{j=1}^{N_{\mathrm{V90}_i}} p_j}{n_{\mathrm{AGN}} \mathrm{V90}_i}$$

$$\mathcal{B}_i = \frac{0.9}{\mathrm{V90}_i}$$

Number of AGN within localisation volumes ✓

Multiple AGN ✓

Size of localisation volumes ✓

Our method

Multiple detected BBH mergers ✓

Incompleteness of AGN catalogues ✓ NEW!

$$\mathcal{L}\left(f_{\mathrm{AGN}}\right) = \prod_{i=1}^{N_{\mathrm{GW}}} \left[c \cdot 0.9 \cdot f_{\mathrm{AGN}} \cdot \mathcal{S}_i + \left(1 - c \cdot 0.90 \cdot f_{\mathrm{AGN}}\right) \mathcal{B}_i\right]$$

Number of AGN within localisation volumes ✓

$$\mathcal{S}_i = \frac{\sum_{j=1}^{N_{\mathrm{V90}_i}} p_j}{n_{\mathrm{AGN}} \mathrm{V90}_i}$$

$$\mathcal{B}_i = \frac{0.9}{\mathrm{V90}_i}$$

Multiple AGN ✓

Size of localisation volumes ✓

Our method

$$\mathcal{L}\left(f_{\rm AGN}\right) = \prod_{i=1}^{N_{\rm GW}} \left[c \cdot 0.9 \cdot f_{\rm AGN} \cdot \mathcal{S}_i + (1 - c \cdot 0.90 \cdot f_{\rm AGN})\,\mathcal{B}_i\right]$$

$$\mathcal{S}_i = \frac{\sum_{j=1}^{N_{\mathrm{V90}_i}} p_j}{n_{\rm AGN}\,\mathrm{V90}_i} \qquad \mathcal{B}_i = \frac{0.9}{\mathrm{V90}_i}$$

- Multiple detected BBH mergers ✓
- Incompleteness of AGN catalogues ✓ NEW!
- Exact positions of AGN ✓ NEW!
- Number of AGN within localisation volumes ✓
- Multiple AGN ✓
- Size of localisation volumes ✓

Our method

Multiple detected BBH mergers ✓

Incompleteness of AGN catalogues ✓ NEW!

$$\mathcal{L}\left(f_{\mathrm{AGN}}\right)=\prod_{i=1}^{N_{\mathrm{GW}}}\left[c\cdot 0.9\cdot f_{\mathrm{AGN}}\cdot \mathcal{S}_i+\left(1-c\cdot 0.90\cdot f_{\mathrm{AGN}}\right)\mathcal{B}_i\right]$$

Exact positions of AGN ✓ NEW!

$$\mathcal{S}_i=\frac{\sum_{j=1}^{N_{\mathrm{V90}_i}} p_j}{n_{\mathrm{AGN}}\mathrm{V90}_i}$$

$$\mathcal{B}_i=\frac{0.9}{\mathrm{V90}_i}$$

Number of AGN within localisation volumes ✓

Multiple AGN ✓

Size of localisation volumes ✓

Likelihood maximization ($\mathscr{L}(f_{\mathrm{AGN}})$) ✓ NEW!

Our method

Multiple detected BBH mergers

Incompleteness of AGN catalogues NEW!

$$\mathcal{L}\left(f_{\mathrm{AGN}}\right) = \prod_{i=1}^{N_{\mathrm{GW}}} \left[c \cdot 0.9 \cdot f_{\mathrm{AGN}} \cdot \mathcal{S}_i + \left(1 - c \cdot 0.90 \cdot f_{\mathrm{AGN}}\right) \mathcal{B}_i\right]$$

Exact positions of AGN NEW!

Number of AGN within localisation volumes

$$\mathcal{S}_i = \frac{\sum_{j=1}^{N_{\mathrm{V90}_i}} p_j}{n_{\mathrm{AGN}} \mathrm{V90}_i} \qquad \mathcal{B}_i = \frac{0.9}{\mathrm{V90}_i}$$

Multiple AGN

Size of localisation volumes

Likelihood maximization ($\mathscr{L}(f_{\mathrm{AGN}})$) NEW!

Application to observed data NEW!

Results

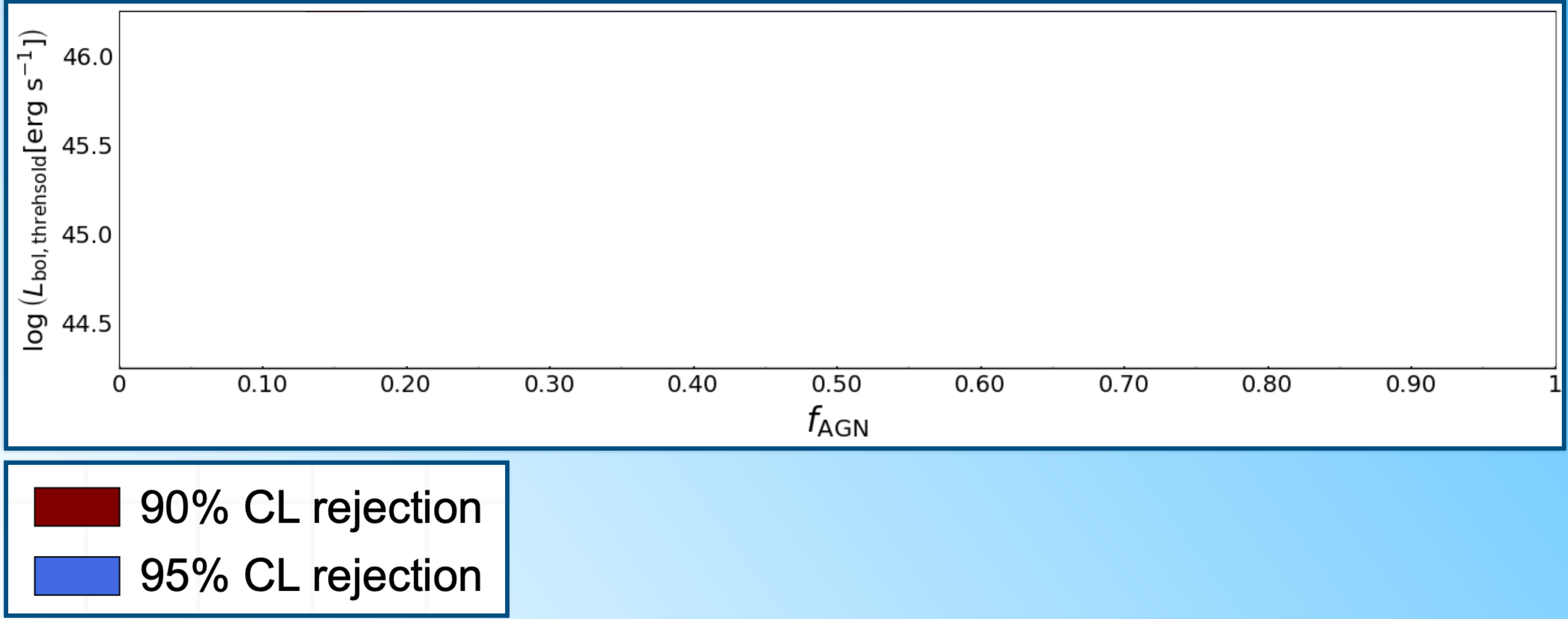

NV+23

Results

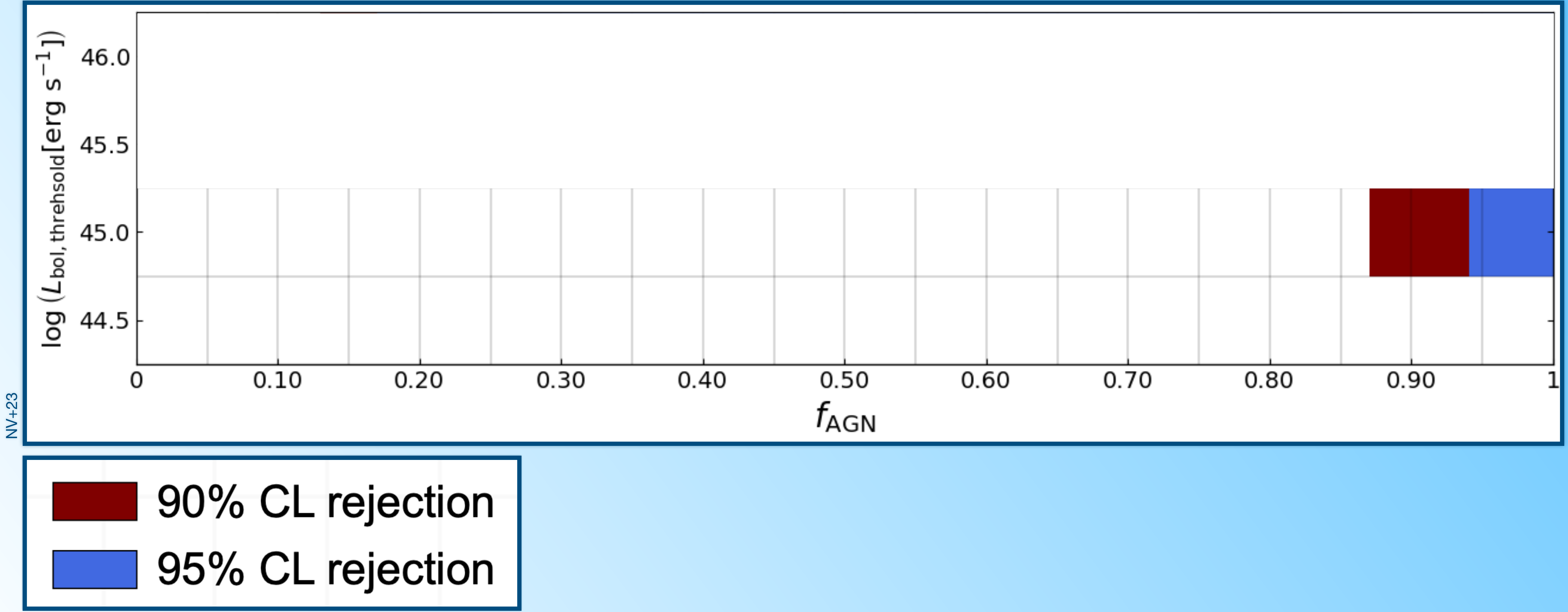

$\log(L_{\rm bol,\,threhsold}\,[\rm erg\ s^{-1}])$
46.0
45.5
45.0
44.5
0
0.10
0.20
0.30
0.40
0.50
0.60
0.70
0.80
0.90
1
$f_{\rm AGN}$
NV+23
90% CL rejection
95% CL rejection

Results

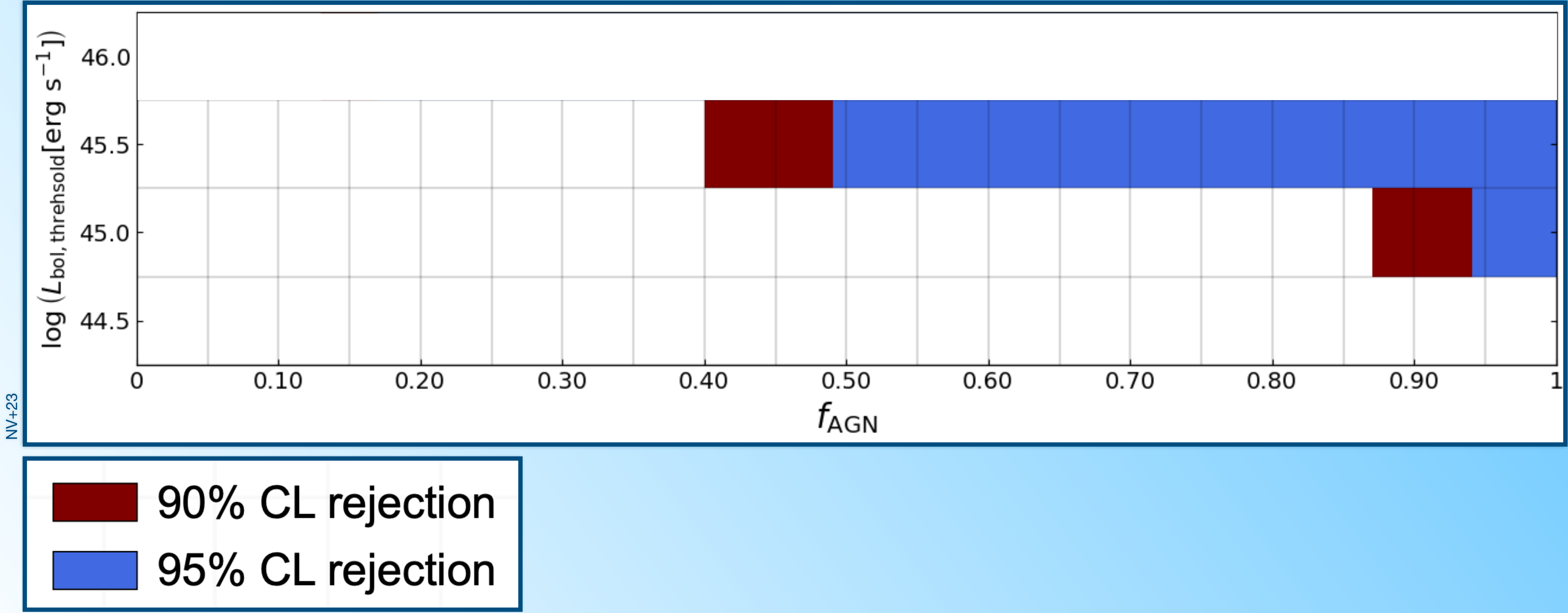

NV+23
log ($L_{bol, threhsold}$ [erg s^{-1}])
46.0
45.5
45.0
44.5
0
0.10
0.20
0.30
0.40
0.50
0.60
0.70
0.80
0.90
1
f_{AGN}
90% CL rejection
95% CL rejection

Results

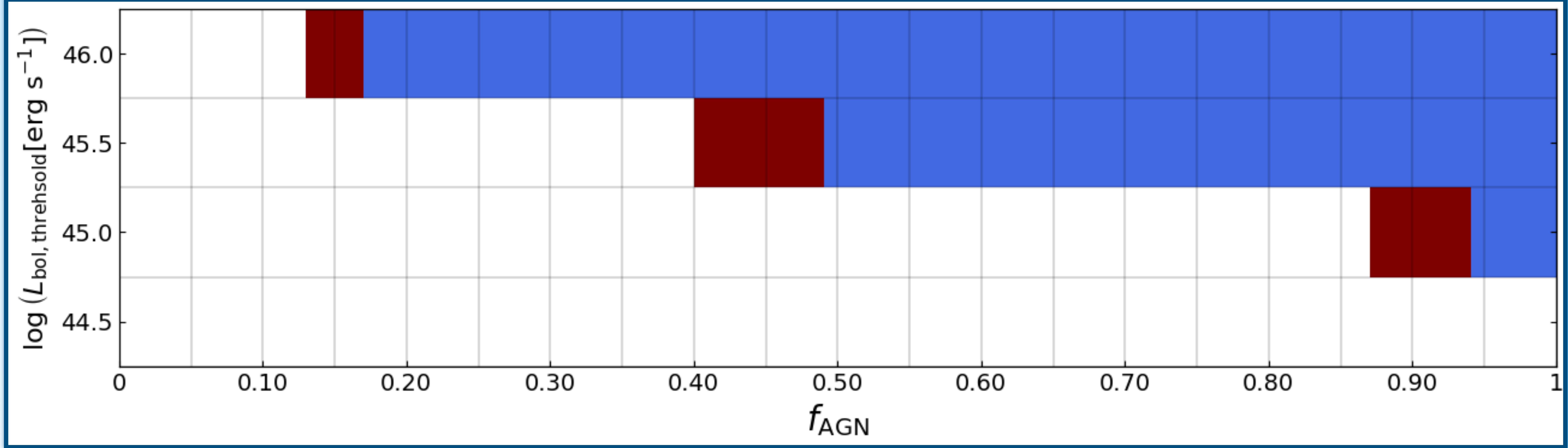

NV+23

90% CL rejection

95% CL rejection

Results

Observations

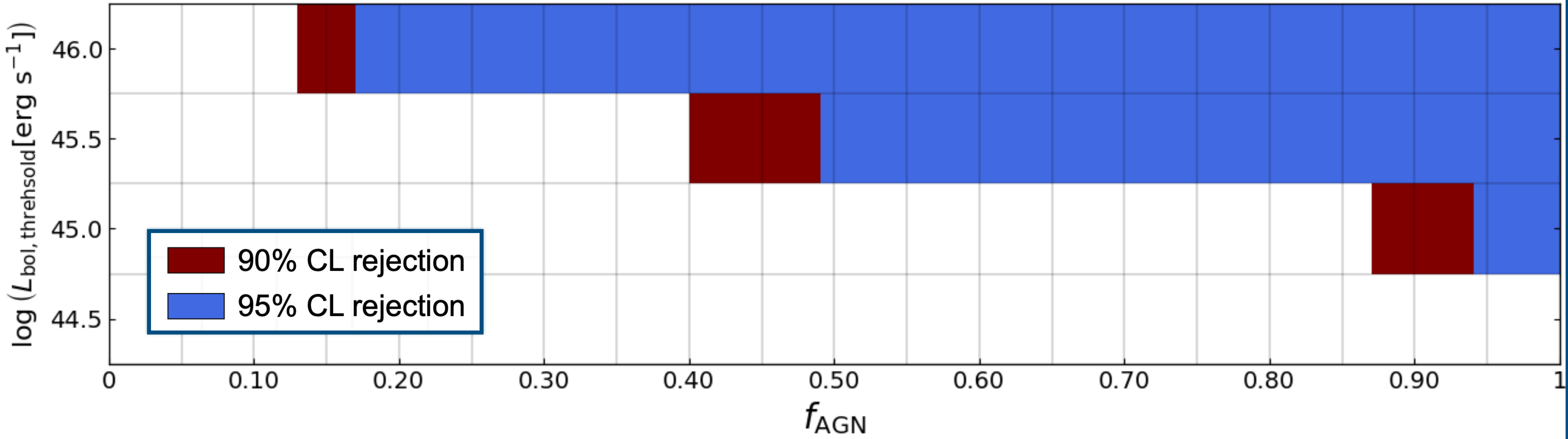

NV+23

Theory

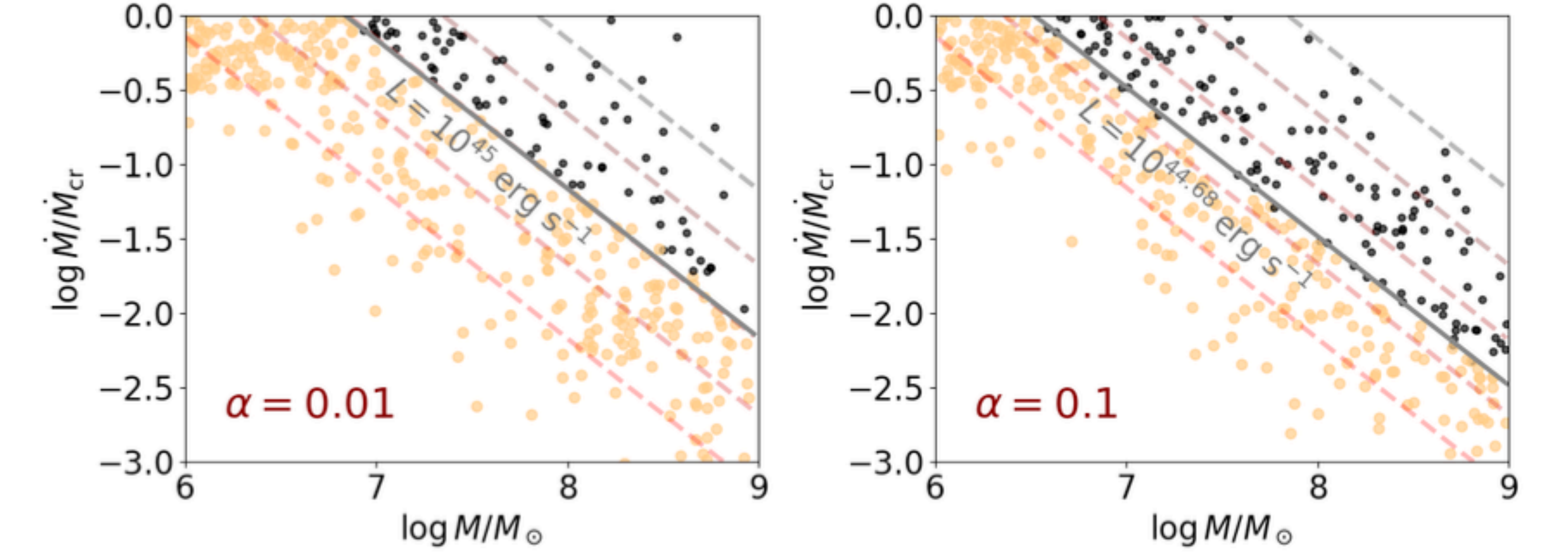

Figure 10. The dichotomous range of AGN migration traps in $\{M, \dot{M}\}$ space. The large orange points are discs that have traps, while the small black points are discs that do not. The dashed curves are lines of constant $L_{\rm AGN}$ from 10^{44} erg s^{-1} to 10^{46} erg s^{-1} in jumps of 0.5 dex. The thick grey line is the approximate bifurcation boundary between discs that have traps and discs that do not. *Left panel*: $\alpha = 0.01$. *Right panel*: $\alpha = 0.1$. The highest luminosity AGN lack migration traps.

Grishin+23

Future perspectives

Future perspectives

Future perspectives

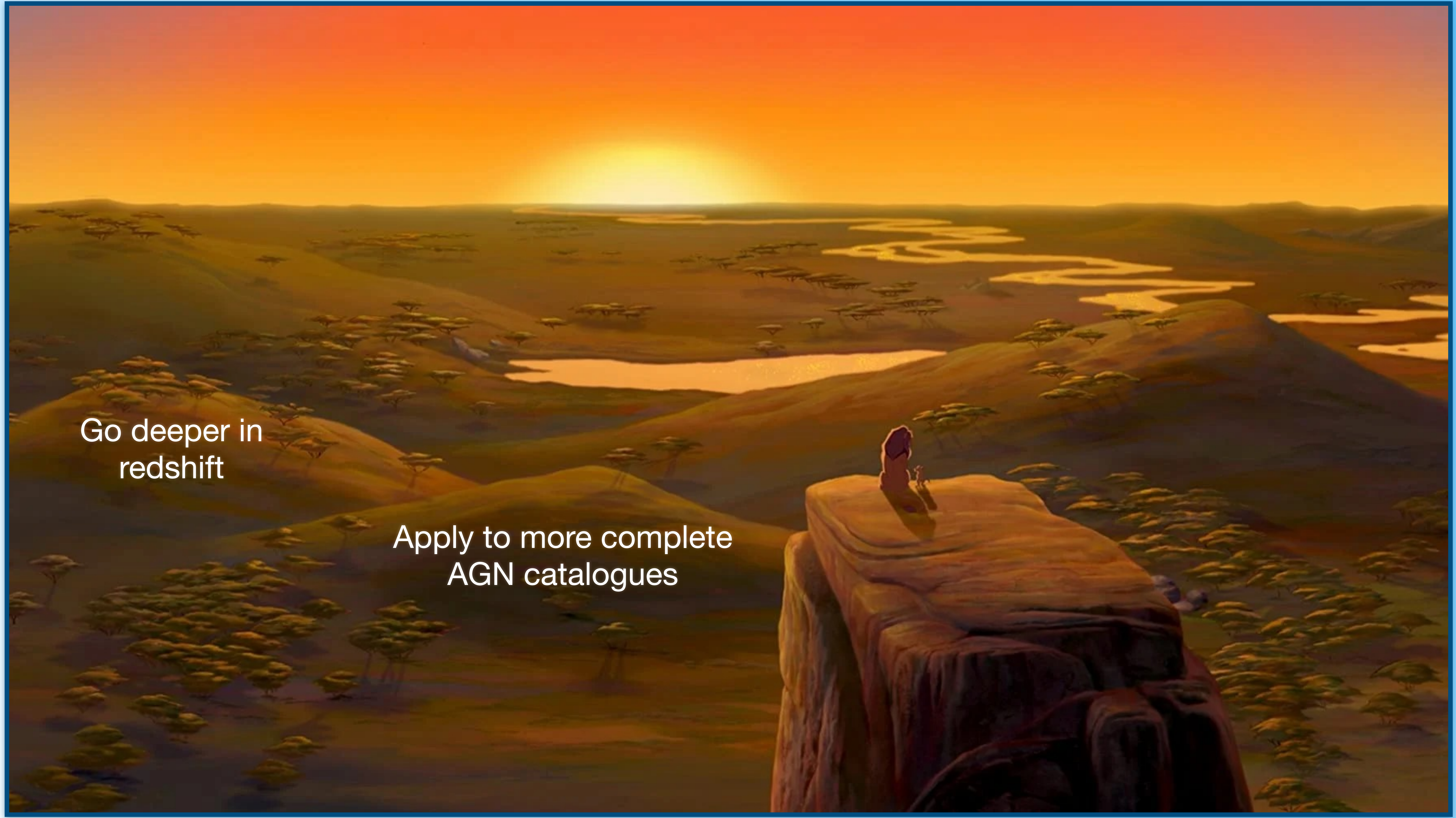

Future perspectives

Future perspectives

Future perspectives

Future perspectives

Future perspectives

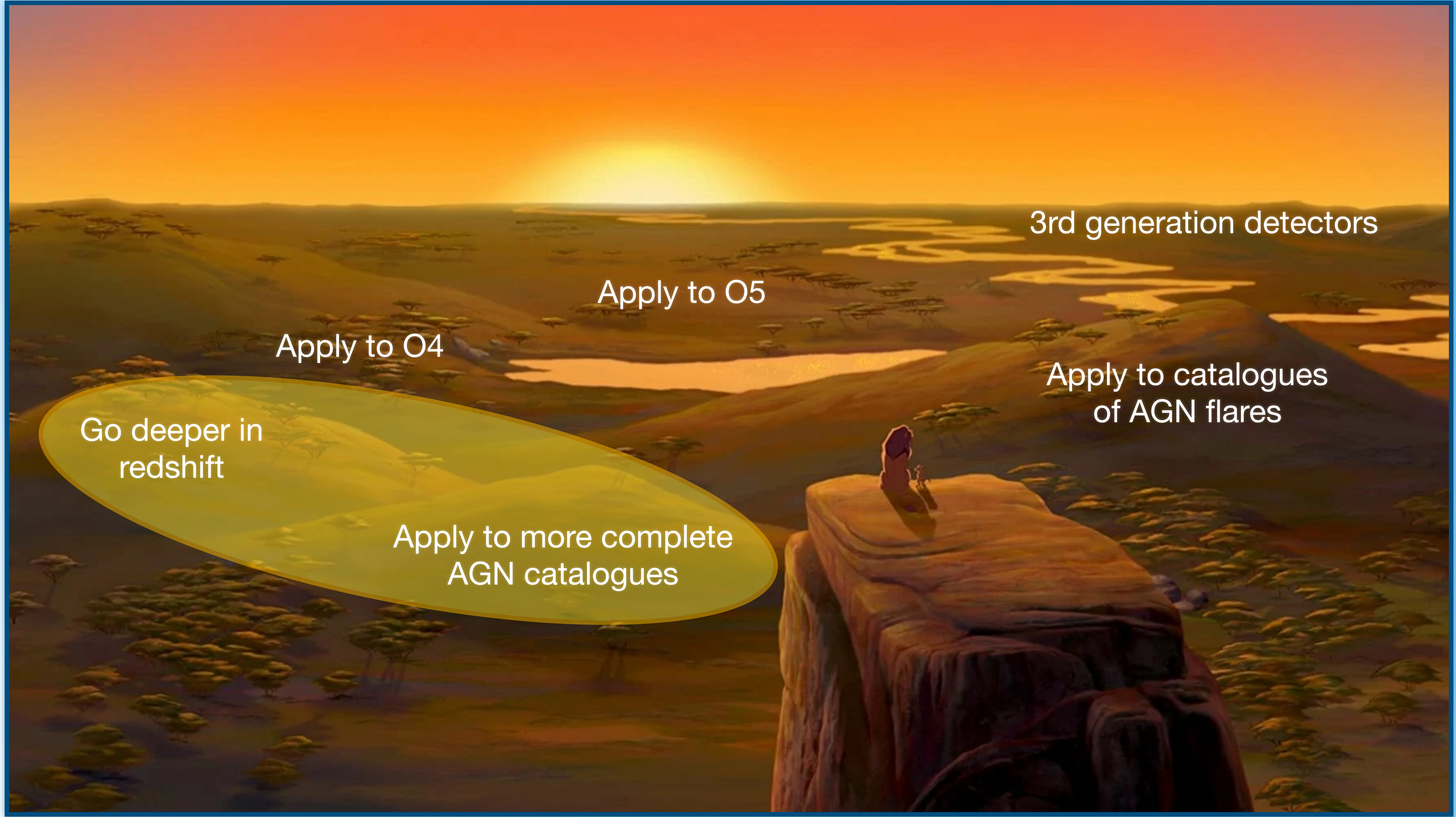

Future perspectives

Go deeper in redshift

Apply to more complete AGN catalogues

Quaia, the *Gaia–unWISE* Quasar Catalog: An All-Sky Spectroscopic Quasar Sample

Kate Storey-Fisher [1] David W. Hogg [1,2,3] Hans-Walter Rix [3] Anna-Christina Eilers [4]
Giulio Fabbian [5,6] Michael Blanton [1] and David Alonso [7]

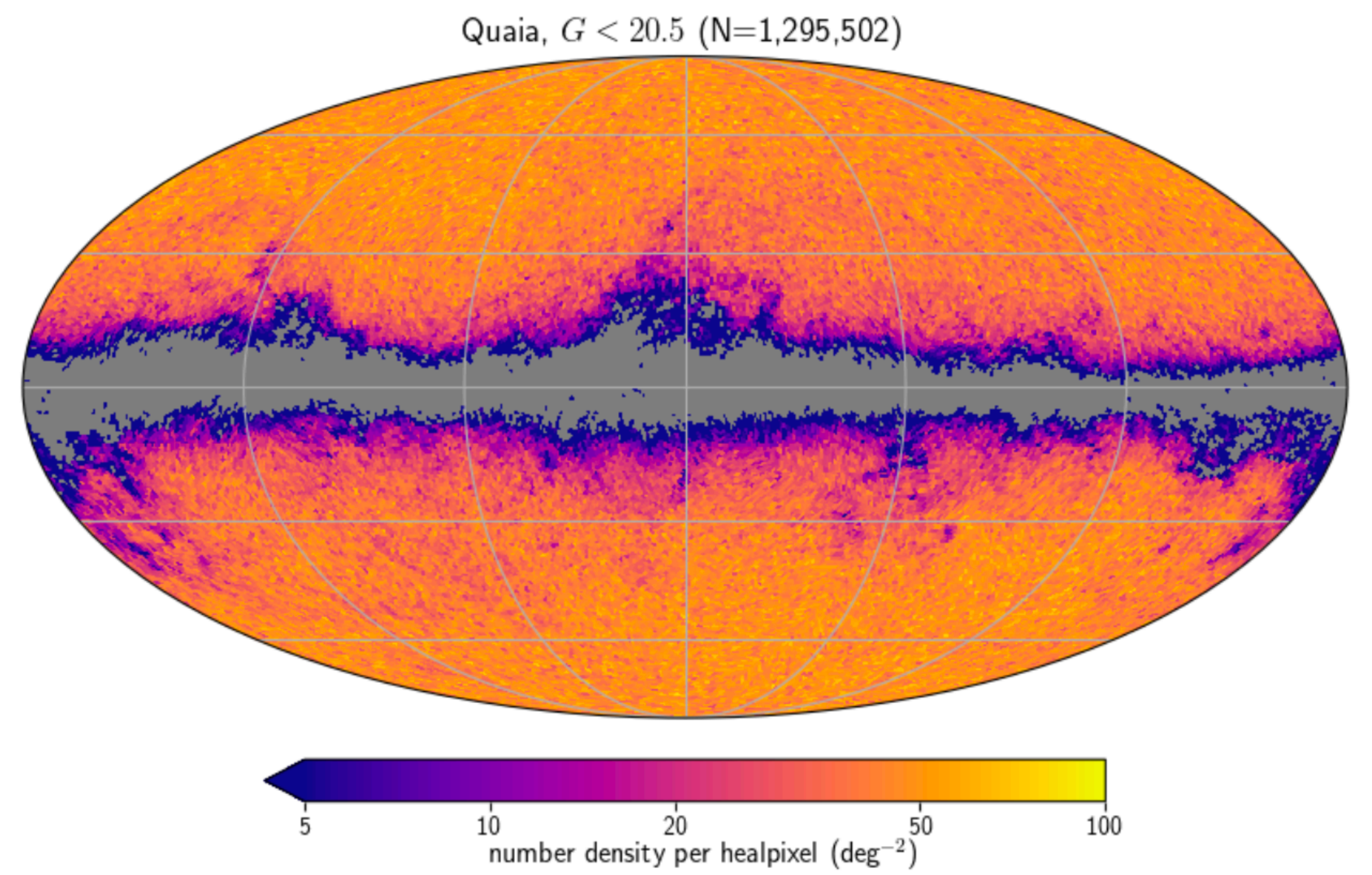

Thank you for your attention!

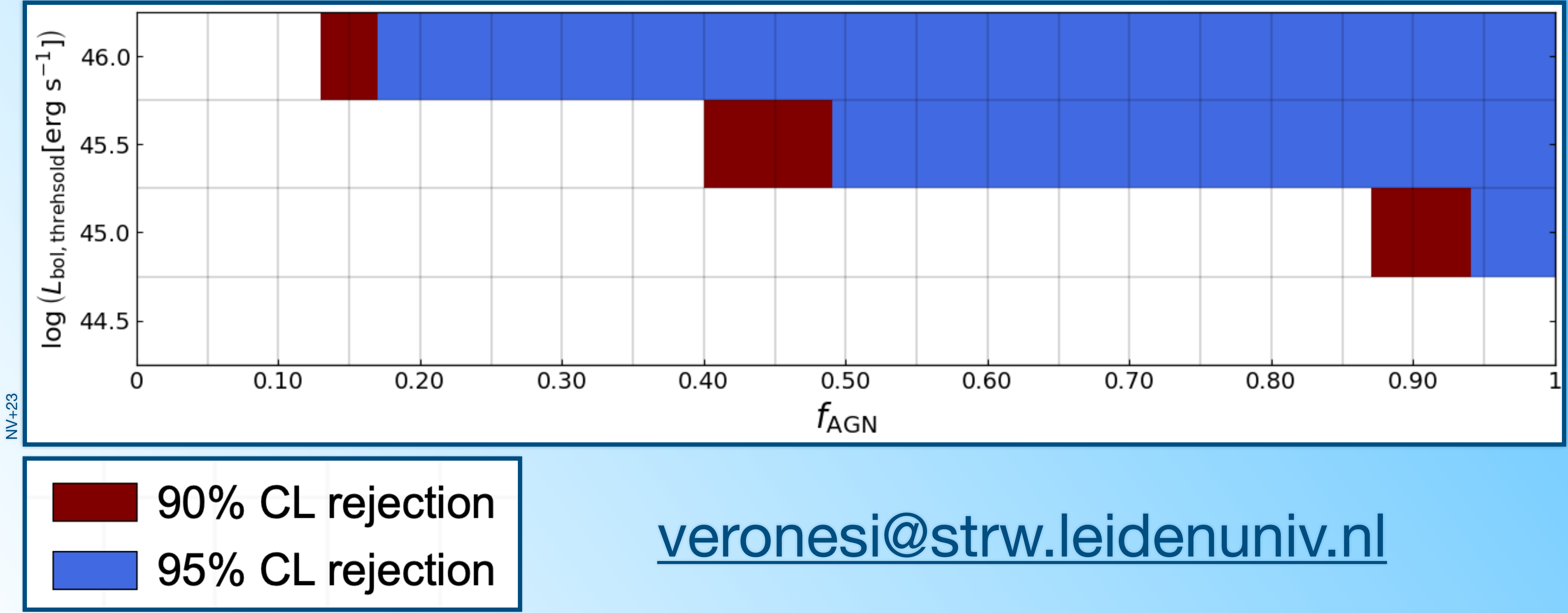

veronesi@strw.leidenuniv.nl

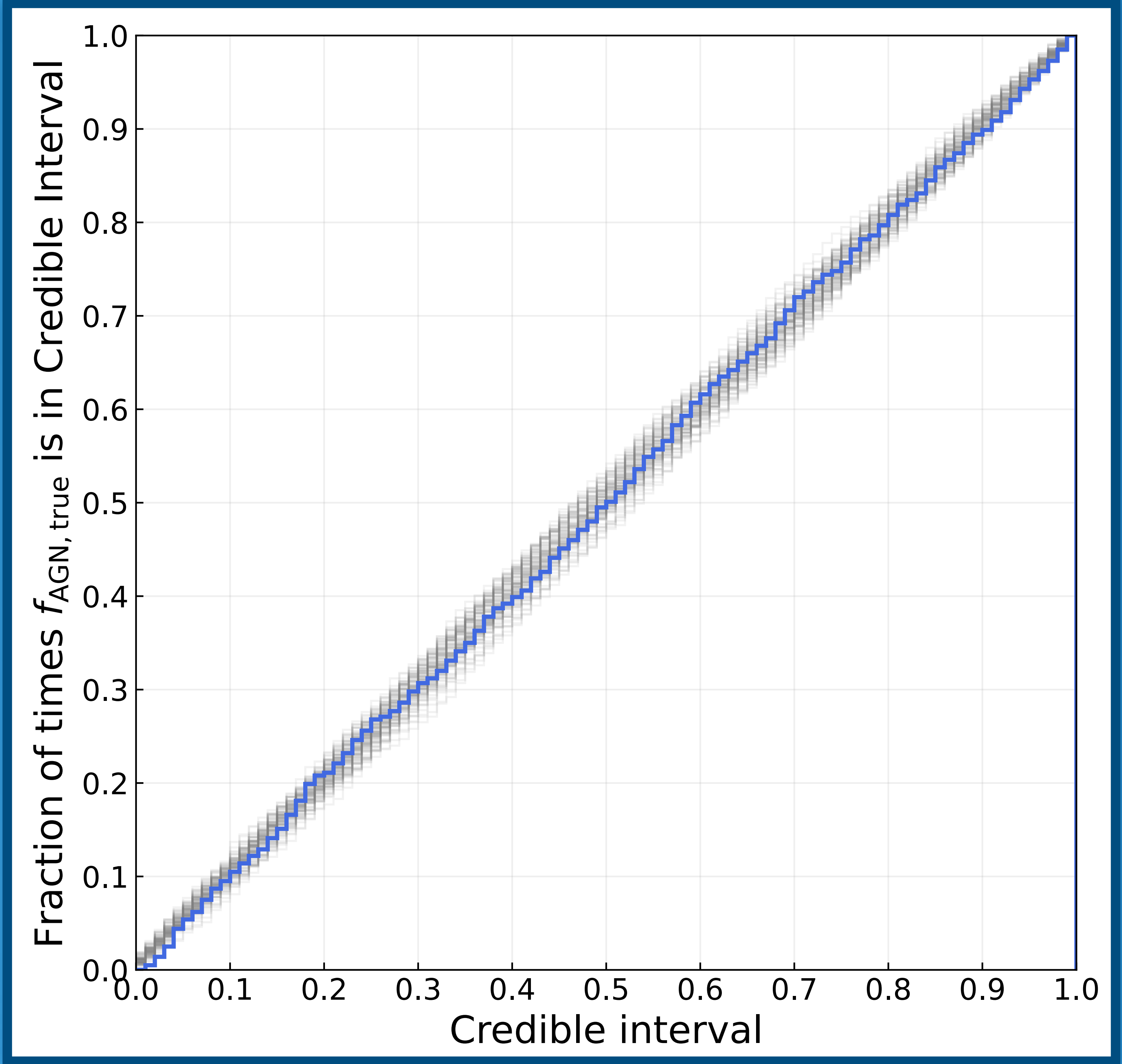

NV+23

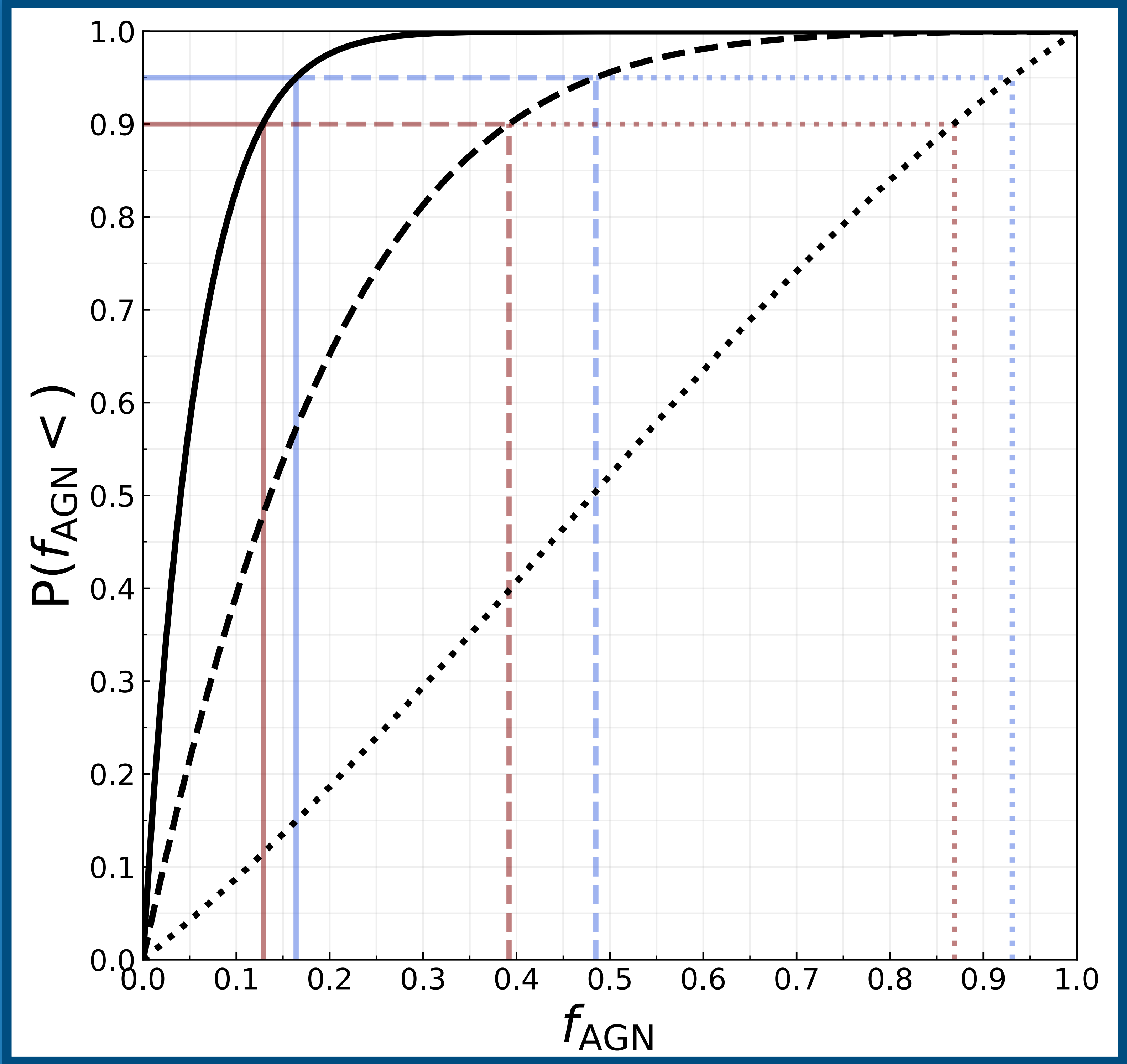

NV+23

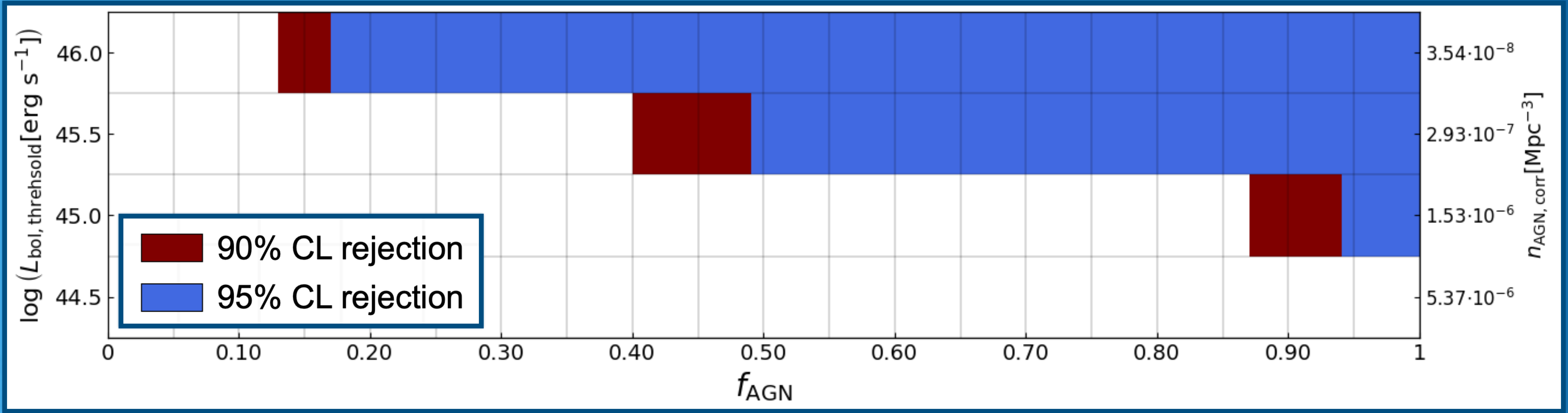

NV+23

Name	Citation for Name	unWISE ID [deg]	R.A. [deg]	Dec.	z	Citation for z	W1 mag	L_{W1} [$erg\,s^{-1}$]
UVQSJ000000.15-200427.7	Monroe et al. (2016)	0000m197o0005716	0.00065	−20.07433	0.291	Monroe et al. (2016)	13.65	$2.72 \cdot 10^{44}$
SDSS J000005.49+310527.6	Ahumada et al. (2020)	0000p318o0001234	0.02290	31.09102	0.286	Ahumada et al. (2020)	14.20	$1.58 \cdot 10^{44}$
PHL 2525	Lamontagne et al. (2000)	0000m122o0001902	0.10172	−12.76328	0.200	Lamontagne et al. (2000)	11.04	$1.29 \cdot 10^{45}$
2MASX J00004028-0541012	Masci et al. (2010)	0000m061o0015237	0.16774	−5.68361	0.094	Masci et al. (2010)	11.33	$1.90 \cdot 10^{44}$
RXS J00009+1723	Wei et al. (1999)	0000p166o0024250	0.23319	17.39413	0.215	Wei et al. (1999)	12.93	$2.64 \cdot 10^{44}$
SDSS J000102.18-102326.9	Lyke et al. (2020)	0000m107o0014745	0.25911	−10.39078	0.294	Lyke et al. (2020)	14.75	$1.01 \cdot 10^{44}$
RX J00013+0728	Tesch & Engels (2000)	0000p075o0010333	0.32534	7.47432	0.270	Tesch & Engels (2000)	14.06	$1.57 \cdot 10^{44}$
PGC 929358	Paturel et al. (2003)	0000m137o0004668	0.33219	−14.07310	0.087	Mauch & Sadler (2007)	11.65	$1.21 \cdot 10^{44}$
PGC 1698547	Paturel et al. (2003)	0000p242o0009501	0.38474	24.04179	0.104	Ahumada et al. (2020)	11.72	$1.65 \cdot 10^{44}$
RX J00015+0529	Tesch & Engels (2000)	0000p060o0003070	0.38896	5.48926	0.250	Ahumada et al. (2020)	12.67	$4.71 \cdot 10^{44}$

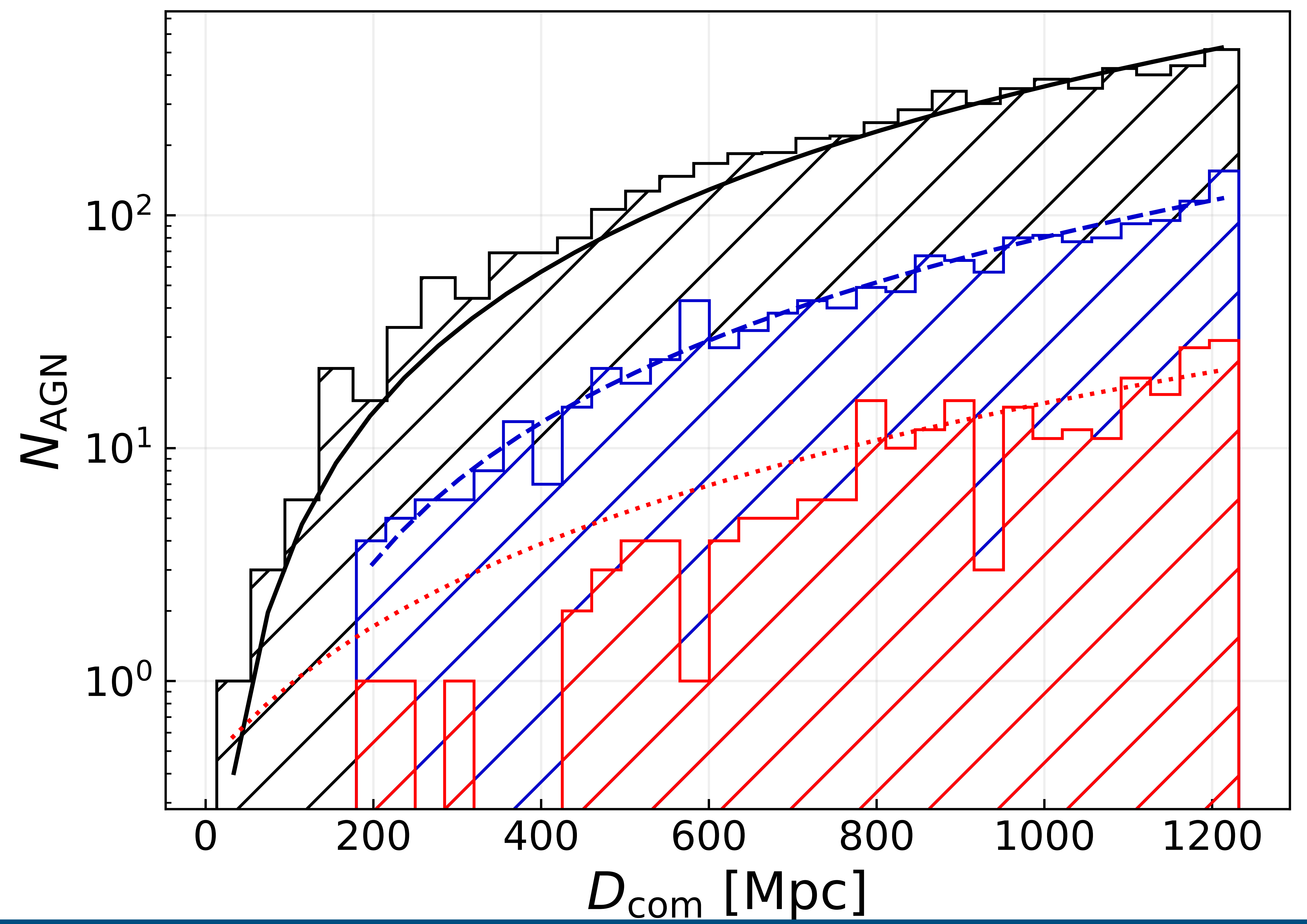

NV+23

Event ID	m_1 $M_\odot$	m_2 $M_\odot$	χ_{eff}	z	SNR	V90 $[Mpc^3]$	$N_{V90,CAT450}$	$N_{V90,CAT455}$	$N_{V90,CAT460}$
GW150914_095045	$34.6^{+4.4}_{-2.6}$	$30.0^{+2.9}_{-4.6}$	$-0.04^{+0.12}_{-0.14}$	$0.10^{+0.03}_{-0.03}$	$26.0^{+0.1}_{-0.2}$	$3.39 \cdot 10^6$	3	0	0
GW151226_033853	$14.2^{+11.1}_{-3.6}$	$7.5^{+2.4}_{-2.8}$	$0.20^{+0.23}_{-0.08}$	$0.10^{+0.03}_{-0.04}$	$12.7^{+0.3}_{-0.4}$	$1.32 \cdot 10^7$	10	1	0
GW170104_101158	$28.7^{+6.6}_{-4.2}$	$20.8^{+4.1}_{-4.7}$	$-0.04^{+0.15}_{-0.19}$	$0.22^{+0.07}_{-0.09}$	$13.8^{+0.2}_{-0.3}$	$1.42 \cdot 10^8$	196	30	6
GW170608_020116	$10.6^{+4.0}_{-1.4}$	$7.8^{+1.2}_{-1.9}$	$0.05^{+0.13}_{-0.05}$	$0.07^{+0.03}_{-0.03}$	$15.3^{+0.2}_{-0.3}$	$2.98 \cdot 10^6$	3	0	0
GW170809_082821	$34.1^{+8.0}_{-5.3}$	$24.2^{+4.8}_{-5.3}$	$0.07^{+0.17}_{-0.17}$	$0.21^{+0.05}_{-0.07}$	$12.8^{+0.2}_{-0.3}$	$4.21 \cdot 10^7$	35	6	1
GW170814_103043	$30.9^{+5.4}_{-3.3}$	$24.9^{+3.0}_{-4.0}$	$0.08^{+0.13}_{-0.12}$	$0.13^{+0.03}_{-0.05}$	$17.7^{+0.2}_{-0.3}$	$2.96 \cdot 10^6$	2	0	0
GW170818_022509	$34.8^{+6.5}_{-4.2}$	$27.6^{+4.1}_{-5.1}$	$-0.06^{+0.19}_{-0.22}$	$0.21^{+0.07}_{-0.07}$	$12.0^{+0.3}_{-0.4}$	$6.04 \cdot 10^6$	3	1	0
GW190412_053044	$27.7^{+6.0}_{-6.0}$	$9.0^{+2.0}_{-1.4}$	$0.21^{+0.12}_{-0.13}$	$0.15^{+0.04}_{-0.04}$	$19.8^{+0.2}_{-0.3}$	$9.16 \cdot 10^6$	20	3	0
GW190425_081805	$2.1^{+0.5}_{-0.4}$	$1.3^{+0.3}_{-0.2}$	$0.07^{+0.07}_{-0.05}$	$0.03^{+0.02}_{-0.01}$	$12.4^{+0.4}_{-0.4}$	$7.78 \cdot 10^6$	9	1	0
GW190630_185205	$35.1^{+6.5}_{-5.5}$	$24.0^{+5.5}_{-5.2}$	$0.10^{+0.14}_{-0.13}$	$0.18^{+0.09}_{-0.07}$	$16.4^{+0.2}_{-0.3}$	$1.23 \cdot 10^8$	148	33	4
GW190707_093326	$12.1^{+2.6}_{-2.0}$	$7.9^{+1.6}_{-1.3}$	$-0.04^{+0.10}_{-0.09}$	$0.17^{+0.06}_{-0.08}$	$13.1^{+0.2}_{-0.4}$	$9.20 \cdot 10^7$	17	3	1
GW190708_232457	$19.8^{+4.3}_{-4.3}$	$11.6^{+3.1}_{-2.0}$	$0.05^{+0.10}_{-0.10}$	$0.19^{+0.06}_{-0.07}$	$13.4^{+0.2}_{-0.3}$	$1.02 \cdot 10^9$	1560	305	43
GW190720_000836	$14.2^{+5.6}_{-3.3}$	$7.5^{+2.2}_{-1.8}$	$0.19^{+0.14}_{-0.11}$	$0.16^{+0.11}_{-0.05}$	$10.9^{+0.3}_{-0.8}$	$4.24 \cdot 10^7$	20	7	1
GW190725_174728	$11.8^{+10.1}_{-3.0}$	$6.3^{+2.1}_{-2.5}$	$-0.04^{+0.36}_{-0.16}$	$0.20^{+0.09}_{-0.08}$	$9.1^{+0.4}_{-0.7}$	$3.81 \cdot 10^8$	106	44	11
GW190728_064510	$12.5^{+6.9}_{-2.3}$	$8.0^{+1.7}_{-2.6}$	$0.13^{+0.19}_{-0.07}$	$0.18^{+0.05}_{-0.07}$	$13.1^{+0.3}_{-0.4}$	$3.88 \cdot 10^7$	17	4	0
GW190814_211039	$23.3^{+1.4}_{-1.4}$	$2.6^{+0.1}_{-0.1}$	$0.00^{+0.07}_{-0.07}$	$0.05^{+0.01}_{-0.01}$	$25.3^{+0.1}_{-0.2}$	$3.55 \cdot 10^4$	0	0	0
GW190917_033853	$9.7^{+3.4}_{-3.9}$	$2.1^{+1.1}_{-0.4}$	$-0.08^{+0.21}_{-0.43}$	$0.15^{+0.05}_{-0.06}$	$8.3^{+0.5}_{-0.8}$	$1.05 \cdot 10^8$	60	22	3
GW190924_021846	$8.8^{+4.3}_{-1.8}$	$5.1^{+1.2}_{-1.5}$	$0.03^{+0.20}_{-0.08}$	$0.11^{+0.04}_{-0.04}$	$12.0^{+0.3}_{-0.4}$	$1.27 \cdot 10^7$	13	1	0
GW190925_232845	$20.8^{+6.5}_{-2.9}$	$15.5^{+2.5}_{-3.6}$	$0.09^{+0.16}_{-0.15}$	$0.19^{+0.08}_{-0.07}$	$9.7^{+0.3}_{-0.6}$	$2.86 \cdot 10^8$	401	94	12
GW190930_133541	$14.2^{+8.0}_{-4.0}$	$6.9^{+2.4}_{-2.1}$	$0.19^{+0.22}_{-0.16}$	$0.16^{+0.06}_{-0.06}$	$9.7^{+0.3}_{-0.5}$	$1.32 \cdot 10^8$	63	13	2
GW191103_022549	$11.8^{+6.2}_{-2.2}$	$7.9^{+1.7}_{-2.4}$	$0.21^{+0.16}_{-0.10}$	$0.20^{+0.09}_{-0.09}$	$8.9^{+0.3}_{-0.5}$	$3.16 \cdot 10^8$	255	62	8
GW191105_143512	$10.7^{+3.7}_{-1.6}$	$7.7^{+1.4}_{-1.9}$	$-0.02^{+0.13}_{-0.09}$	$0.23^{+0.07}_{-0.09}$	$9.7^{+0.3}_{-0.5}$	$1.53 \cdot 10^8$	164	36	3
GW191129_134029	$10.7^{+4.1}_{-2.1}$	$6.7^{+1.5}_{-1.7}$	$0.06^{+0.16}_{-0.08}$	$0.16^{+0.05}_{-0.06}$	$13.1^{+0.2}_{-0.3}$	$5.92 \cdot 10^7$	101	20	2
GW191204_171526	$11.9^{+3.3}_{-1.8}$	$8.2^{+1.4}_{-1.6}$	$0.16^{+0.08}_{-0.05}$	$0.13^{+0.04}_{-0.05}$	$17.5^{+0.2}_{-0.2}$	$1.24 \cdot 10^7$	12	1	0
GW191216_213338	$12.1^{+4.6}_{-2.3}$	$7.7^{+1.6}_{-1.9}$	$0.11^{+0.13}_{-0.06}$	$0.07^{+0.02}_{-0.03}$	$18.6^{+0.2}_{-0.2}$	$3.66 \cdot 10^6$	2	2	0
GW200115_042309	$5.9^{+2.0}_{-2.5}$	$1.44^{+0.85}_{-0.29}$	$-0.15^{+0.24}_{-0.42}$	$0.06^{+0.09}_{-0.02}$	$11.3^{+0.3}_{-0.5}$	$3.79 \cdot 10^6$	3	2	0
GW200129_065458	$34.5^{+9.9}_{-3.2}$	$28.9^{+3.4}_{-9.3}$	$0.11^{+0.11}_{-0.16}$	$0.18^{+0.05}_{-0.07}$	$26.8^{+0.2}_{-0.2}$	$7.06 \cdot 10^6$	7	0	0
GW200202_153413	$10.1^{+3.5}_{-1.4}$	$7.3^{+1.1}_{-1.7}$	$0.04^{+0.13}_{-0.66}$	$0.09^{+0.03}_{-0.03}$	$10.8^{+0.2}_{-0.4}$	$2.32 \cdot 10^6$	2	0	0
GW200311_115853	$34.2^{+6.4}_{-3.8}$	$27.7^{+4.1}_{-5.9}$	$-0.02^{+0.16}_{-0.20}$	$0.23^{+0.05}_{-0.07}$	$17.8^{+0.2}_{-0.2}$	$5.94 \cdot 10^6$	7	2	0
GW200316_215756	$13.1^{+10.2}_{-2.9}$	$7.8^{+1.9}_{-2.9}$	$0.13^{+0.27}_{-0.10}$	$0.22^{+0.08}_{-0.08}$	$10.3^{+0.4}_{-0.7}$	$9.22 \cdot 10^7$	12	5	0

The Effect of Thermal Torques on AGN Disc Migration Traps and Gravitational Wave Populations

Evgeni Grishin ,[1,2]* Shmuel Gilbaum[3], and Nicholas C. Stone[3]
[1] *School of Physics and Astronomy, Monash University, Clayton, VIC 3800, Australia*
[2] *The ARC Centre of Excellence for Gravitational Wave Discovery – OzGrav, Clayton, VIC 3800, Australia*
[3] *Racah Institute of Physics, The Hebrew University, Jerusalem, 91904, Israel*

18 July 2023

ABSTRACT
Accretion discs in active galactic nuclei (AGN) foster black hole (BH) formation, growth, and mergers. Stellar mass BHs migrate inwards under the influence of hydrodynamical torques unless they encounter a region where the torque flips sign. At these migration traps, BHs accumulate and merge via dynamical or gas-assisted interactions, producing high-frequency LIGO/Virgo/KAGRA (LVK) gravitational wave (GW) sources and potentially cutting off the supply of extreme mass ratio inspirals that would otherwise make low-frequency, *LISA*-band GWs. In this paper, we study the interplay between different types of migration torques, focusing especially on the "thermal torques" generated by the thermal response of the AGN to embedded stellar-mass BHs that accrete through their own mini-discs. In contrast to previous work, we find that Type I torques cannot produce migration traps on their own, but thermal torques often do, particularly in low-mass AGN. The migration traps produced by thermal torques exist at much larger distances ($\sim 10^{3-5}$ gravitational radii) than do previously identified Type I traps, carrying implications for GW populations at multiple frequencies. Finally, we identify a bifurcation of AGN discs into two regimes: migration traps exist below a critical AGN luminosity, and do not at higher luminosities. This critical luminosity is fit as $\log_{10} L^c_{\rm AGN} = 45 - 0.32 \log_{10}(\alpha/0.01)$ where α is the Shakura-Sunyaev viscosity parameter, a range compatible with recent claims that LVK GWs are not preferentially associated with high-luminosity AGN.